The Relationship of the North American Monsoon to Tropical and North Pacific Sea Surface Temperatures as Revealed by Observational Analyses

Christopher L. Castro
Thomas B. McKee
Roger A. Pielke, Sr.

Colorado State University

Climatology Report No. 00-1

DEPARTMENT OF ATMOSPHERIC SCIENCE

PAPER NO. 693

THE RELATIONSHIP OF THE NORTH AMERICAN MONSOON TO TROPICAL AND NORTH PACIFIC SEA SURFACE TEMPERATURES AS REVEALED BY OBSERVATIONAL ANALYSES

Christopher L. Castro

Thomas B. McKee

Roger A. Pielke, Sr.

Department of Atmospheric Science
Colorado State University
Fort Collins, Colorado

April 2000

Atmospheric Science Paper No. 693

ABSTRACT

THE RELATIONSHIP OF THE NORTH AMERICAN MONSOON TO TROPICAL AND NORTH PACIFIC SEA SURFACE TEMPERATURES AS REVEALED BY OBSERVATIONAL ANALYSES

The North American Monsoon is a seasonal shift of upper and low level pressure and wind patterns which brings summertime moisture into the Southwest United States and ends the late spring wet period in the Great Plains. The climatology and interannual variability of the North American Monsoon are examined using the NCEP/NCAR Reanalysis (1948-98). The diurnal and seasonal evolution of 500-mb geopotential height , integrated moisture flux, and integrated moisture flux convergence are constructed using a five-day running mean for the months May through September. All of the years are used to calculate an average daily Z-score which removes the diurnal, seasonal, and intraseasonal variability. The average Z-score centered about the date is correlated with three Pacific SST indices associated with the El Niño Southern Oscillation (ENSO) and the North Pacific Oscillation (NPO). These indices are: Niño 3, a North Pacific index, and a North American Monsoon index (M) which combines the previous two. Regional time evolving precipitation indices for the Southwest and Great Plains, which consider the total number of wet or dry stations in a region, are also correlated with the SST indices. The new reanalysis climatology reveals: the time of maximum northward extent of the monsoon is late July, a diurnal cycle in atmospheric moisture which reflects the evolution of summer thunderstorms, the presence of the Baja and Great Plains low level jets, and the seasonal dependence of

atmospheric moisture on monsoon ridge position. These results are in agreement with previous, more comprehensive reanalysis climatologies using shorter lengths of record.

Pacific SSTs are related to a sequence of teleconnection patterns over North America through the summer. The relationship to the atmospheric circulation is strongest at monsoon onset, when the Pacific Transition pattern controls the large-scale distribution of moisture across the western U.S. A high (low) NPO phase and El Niño (La Niña) conditions favor a trough (ridge) over the northern Rocky Mountains, northern Great Plains. In the Great Plains the spring wet season is lengthened (shortened) and early summer rainfall and integrated moisture flux convergence are above (below) average. In the Southwest monsoon onset is late (early) and early summer rainfall and integrated moisture flux convergence are below (above) average. Relationships with the Pacific SST indices decay in the later part of the monsoon. These idealized climatological responses associated with high and low values of the M index were observed in the Midwest Flood of 1993 and the Drought of 1988, respectively. Tropical and North Pacific SSTs are related to atmospheric moisture and precipitation in the western U.S. to varying degrees depending on location. In the Great Plains, North Pacific SSTs are dominant factor, while in the Southwest tropical and North Pacific SSTs are equally important. Though the M index is the better diagnostic for North American Monsoon, only the time-coincident relationships with atmospheric circulation and moisture are statistically significant. A statistically significant relationship exists between spring Niño 3 and the atmospheric circulation pattern over North America at monsoon onset.

ACKNOWLEDGMENTS

The authors would like to thank Dr. Freeman Smith from CSU's Natural Resource Department for his review of this paper. They would also like to thank the McKee and Pielke staff members who provided valuable technical and administrative support, including Nolan Doesken, John Kleist, Dr. Glen Liston, Chris Roupp, Odie Bliss, Tara Green, and Dallas McDonald. They also like to acknowledge the support from graduate students Dr. Thomas Chase, Dr. Lixin Lu, and Captain Brian Griffith, USAF.

Many diverse data were accessed for this project. Chi-Fan Shih, of the Scientific Computing Division at the National Center for Atmospheric Research, was most helpful for NCEP/NCAR Reanalysis. Rick Taft of the Atmospheric Science Department here at CSU provided the COADS SST data.

This research was funded through the Significant Opportunities in Atmospheric Research and Science (SOARS) program through the University Corporation for Atmospheric Research (UCAR) and the Cooperative Institute for Research in the Atmosphere (CIRA) through the National Oceanic and Atmospheric Administration (NOAA) for funding my research and graduate studies. In particular, we would like to acknowledge the support from the SOARS coordinators, Dr. Thomas Windham and Ms. Beverly Johnson.

Christopher L. Castro would like to dedicate this work to his father, Dr. Anthony E. Castro, DVM, Ph.D., on the eve of his retirement after more than twenty years of service in animal diagnostics.

TABLE OF CONTENTS

I. INTRODUCTION

The western U.S. is particularly sensitive to interannual variability of summer climate. In the most arid regions of the Southwest U.S., this variability can be larger than mean summer rainfall itself (Higgins et al. 1998). Climate and weather extremes produce unique dangers and their effects vary in scope. Severe weather hazards include high winds, hail, lightning, and tornadoes, especially from supercell thunderstorms in the Great Plains. Flash flooding arises from individual localized summer thunderstorms with high rainfall rates. These events are common the Southwest U.S. because of its steep terrain and poor soil moisture holding capacity. Sustained summer flood or drought conditions over broad areas, such as the Flood of 1993 or the Drought of 1988, result from shifts in the large-scale circulation pattern in summer (e.g.Trenberth and Branstator 1992; Bell and Janowiak1995; Trenberth and Guillemot 1996). Short or long-term departures from average conditions may adversely affect infrastructure, agricultural production, water supply, and hydroelectric power generation. The sensitivity to these extreme conditions is likely to increase in the next century if the current trends of population growth and rapid development in urban areas continue. There is a critical need to understand the causes of interannual variability so seasonal forecasts can be improved.

The North American Monsoon (NAM) controls the large-scale distribution of summer moisture in the western U.S. The NAM is a true monsoon in that elevated heat sources drive a reversal of the circulation in the summer, causing a transport of moisture into western North America. The heating sources are the Colorado Plateau, extending

from the Mogollon Rim of Arizona to the Rocky Mountains of Colorado, and the Mexican Altiplano, between the Sierra Madre Mountains in Mexico (Adams and Comerie 1997; Barlow et al. 1998). Dry mid latitude westerly flow persists until the middle of June. Monsoon onset is associated with a shift in circulation in late June or early July, on average. An extension of the Bermuda high retreats west, initiating light easterly flow at middle and upper levels (above 850-mb) over the Southwest U.S. (Bryson and Lowry 1955; Adams and Comerie 1997; Higgins et al 1997b). A diurnal surface heat low forms over the southwest Arizona and southern California. Two low level jets (LLJ), the Great Plains LLJ and the Baja LLJ, are active at night and early morning to midday, respectively (Douglas 1995; Higgins et al. 1997a).

There is a rapid increase in precipitation which begins in southern Mexico in June, advances northward along the Sierra Madre Mountains, and arrives into the Southwest U.S. by early July (Douglas et al. 1993; Adams and Comerie 1997; Higgins et al. 1997a). Higgins et al. (1998) defined average monsoon onset dates for regions in Mexico and the United States using a regridded hourly precipitation index. They found average onset dates of 7 June, 17 June, and 7 July for Southwest Mexico (SWMEX), Northwest Mexico (NWMEX), and Arizona-New Mexico (AZNM), respectively. NAM precipitation is principally from daily thunderstorms that form over mountain ranges in the morning and intensify in lowlands later in the day. The amount and timing of NAM precipitation change with latitude. Southern Mexico has two peaks of heavy NAM precipitation, as the intertropical convergence zone advances north in June and retreats in September. Southwest U.S. NAM precipitation is much lighter, because of the influence of the midlatitude storm track, and has only one peak in July (Douglas et al. 1993;

Higgins et al. 1997b). The NAM regime in the U.S. persists until approximately mid-September.

NAM moisture comes from the Gulf of Mexico, the Gulf of California, and the Eastern Pacific. At middle and upper levels, easterly winds carry the Gulf of Mexico moisture on the southern side of the monsoon ridge (e.g. Bryson and Lowry 1955). Low level moisture (below 850-mb) from the Gulf of Mexico reaches the Great Plains by the nocturnal Great Plains LLJ, but this moisture cannot penetrate the continental divide (Retian 1957; Rasmussen 1967). West of the continental divide, the Baja LLJ draws low level moisture up the northern Gulf of California by a Gulf surge mechanism (Hales 1972, Brenner, 1974, Adams and Comerie, 1997). The mean summertime circulation accounts for most water vapor transport and virtually all the moisture into the Southwest U.S. comes from the two gulf sources (Schmitz and Mullen 1996; Higgins et. al. 1997b). Moisture from the Eastern Pacific and Gulf of California is important for convection along the Sierra Madre Occidental in Mexico (Douglas et al. 1993). Though not part of the NAM per se, Eastern Pacific tropical systems are an important secondary source of moisture in late summer. Tropical systems which form off the west coast of Mexico may recurve into northwest Mexico or the Southwest U.S. from late July through September (Kimberlain and Landsea, in press).

In the U.S., the NAM is traditionally defined in the Southwest, namely Arizona and New Mexico. The northern parts of Chihuahua and Sonora in Mexico also may be included climatologically as part of the Southwest. Most NAM studies in the U.S. focus exclusively on this region because of its clear monsoon signature. Hot and dry conditions switch to cooler and wet near the same date annually. However, the shift in circulation

also affects the precipitation in the Great Plains in an opposite way. Formation of the monsoon ridge over the Colorado Plateau causes the Great Plains LLJ to subside and precipitation to decrease in the Great Plains after the middle of June (e.g. Higgins et al. 1997b; Barlow et al. 1998). In this study, we broaden the traditional region of NAM influence in the U.S. to consider climate variability in the both the Great Plains and the Southwest.

Interannual variability of winter precipitation in the western United States has a well-established connection to the El Niño Southern Oscillation (ENSO). Numerous model and observational studies confirm that variations in the location and strength of tropical convection produce coherent teleconnection patterns in the large-scale circulation over North America, specifically the Pacific North America, West Pacific, and Tropical Northern Hemisphere, and North Pacific patterns (e.g. Horel and Wallace 1981; Livezey and Mo 1987). The recognition of these ENSO-associated teleconnections and their associated climate patterns has substantially improved the accuracy of long-range seasonal forecasts for the winter season. El Niño winters are typically dry and warm in the Pacific Northwest and wet in the Southwest. By constrast, La Niña winters are wet in the Pacific Northwest and dry in the Southwest (e.g. Ropelewski and Halpert 1986).

The North Pacific Oscillation (NPO) or, alternatively, the Pacific Decadal Oscillation (PDO), modulates the ENSO teleconnections in winter. The NPO is a quasi-decadal variation in the strength of the Aleutian low and associated pattern of sea surface temperature anomalies (SSTAs) across the North Pacific (Mantua et al. 1997; Minobe et al. 1997; Gurshunov and Barnett 1998). A high (low) NPO phase is characterized by a strong (weak) Aleutian low, a cold (warm) central North Pacific and warm (cold) eastern

North Pacific. There is a correlation between ENSO and NPO, with high (low) NPO favored in El Niño (La Niña) years (Mantua et al. 1997). Modeling studies suggest that the NPO may be forced through ENSO-associated variations in tropical convection (e.g. Lau and Nath, 1994). However, the exact physical mechanism of the NPO is not yet understood and not the subject of this paper. Using long-term sea level pressure and daily precipitation data, Gurshunov and Barnett (1998) showed that the NPO modulates the winter ENSO response. ENSO-associated teleconnection patterns and climate anomalies are most likely when El Niño (La Niña) corresponds with its favored NPO phase. Destructive combinations of ENSO and NPO tend to weaken the effects of either mode of influence, resulting in a weak and incoherent climate response. The NPO was in a high phase, on average, since the late 1970s through most of the 1990s coincident with an increase in frequency of El Niño events.

Most studies of NAM interannual variability, again considering the NAM as affecting the Great Plains and Southwest, follow a standard methodology (e.g. Carleton et al. 1990; Harrington 1992; Hereford and Webb 1992; Bunkers et al., 1996; Gutzler and Preston 1997; Mo et al., 1997; Glenn and Comerie 1998; Higgins et al., 1998; Ting and Wang 1998; Higgins et al. 1999; Higgins and Shi 2000). Summer precipitation is characterized for a given region. Regions are defined by latitude and longitude or similar physiogeographic characteristics. A typical measure of precipitation employed is the normalized departure (or Z-score) from either a seasonal or monthly average over a given area. Interannual variability of precipitation is related to large-scale atmospheric circulation patterns, Pacific sea surface temperature (SST) distributions, or antecedent

land surface conditions, like snow cover. Patterns of correlation or statistically significant differences between wet and dry summers are determined.

Several conclusions can be drawn from the precipitation studies. The monsoon ridge position and strength guide the middle and upper level moisture transport. A relationship between ridge position and interannual variability of NAM rainfall in Arizona was first noted by Carleton et al. (1990). Two configurations of the monsoon ridge exist which can vary in frequency of occurrence either intraseasonally or interannually. In the ridge north configuration, a strong ridge is located over the Great Plains. Upper level easterlies carry moisture from the Gulf of Mexico south of the ridge. The monsoon arrives early and is wet in the Southwest. The Great Plains are dry on the subsiding branch of the ridge. In the ridge south configuration, a trough occurs in the western U.S. and the monsoon ridge is weakened and located over northwest Mexico. Westerly upper level winds over the western U.S. direct moisture into the Great Plains. The Southwest is dry and monsoon onset is delayed. Later studies considering the interannual variability of NAM precipitation in Arizona and New Mexico support this idea (Higgins et al. 1998; Comerie and Glenn 1998; Higgins et al. 1999). The relationship of the monsoon ridge configurations to summer moisture transport, precipitation, and wet and dry summers in the central U.S. is also well established (Mo et al. 1997).

Summer precipitation in the western U.S. is related to the distribution of Pacific SSTs. The relationship is particularly strong in the Great Plains. Bunkers et al. (1996) found statistically significant above (below) average precipitation anomalies over North and South Dakota during El Niño (La Niña) summers. Ting and Wang (1997) correlated

sea surface temperature anomalies (SSTA) in the Pacific with a precipitation index of Great Plains stations. Areas of statistically significant correlation with SSTs in the central and east North Pacific and the equatorial Pacific reflect ENSO and NPO. Using a singular value decomposition technique, they also showed that there are two modes of covariation between Pacific SSTs and Great Plains precipitation, an ENSO mode in the northern Great Plains (and Midwest) and an NPO mode in the southern Great Plains. As a whole, the Great Plains precipitation studies suggest that wet (dry) summers in that region are associated with El Niño (La Niña) and high (low) NPO.

An opposite relationship between Pacific SSTs and NAM precipitation may exist in the Southwest. Carleton et al. (1990) noted in wet monsoons that East Pacific SSTs off the California coast are cooler than average in summer. The enhanced longitudinal temperature gradient between the Eastern Pacific and the Gulf of California increases the strength of the Baja LLJ into the Southwest. In a study using 65 years of monthly precipitation from stations across Arizona and New Mexico, Harrington et al. (1992) found different patterns in summer precipitation for extremes of the Southern Oscillation, with El Niño (La Niña) favoring above average July precipitation in northeast New Mexico (west-central Arizona). Higgins et al. (1999) correlated June-September precipitation totals for three monsoon regions in the U.S. and Mexico with the Southern Oscillation Index (SOI). They found a statistically significant positive (negative) correlation between La Niña (El Niño) and total summer precipitation in southwest Mexico. Higgins et al. (1998) showed that negative SST anomalies in the eastern tropical Pacific during winter and spring are associated with wet monsoons in Arizona and New Mexico. Higgins and Shi (2000) have related the NAM onset and precipitation in the

Southwest U.S. to decade-scale fluctuations in North Pacific SSTs associated with the NPO.

Land surface conditions may affect the summer atmospheric circulation and provide a "memory" of antecedent, ENSO-related winter climate patterns. Modeling studies confirm that antecedent land surface conditions may affect summer temperature, cloudiness, and precipitation on the regional and local scale, especially monsoons (e.g. Anthes and Kuo 1986; Dirmeyer 1994; Meehl, 1994; Sud, 1995). Soil moisture, vegetation, and snow cover affect partitioning of energy at the surface between sensible and latent heat fluxes. Namias (1960) first suggested that dry, warm spring conditions in the Great Plains leads to a greater sensible heat flux and enhancement of the monsoon ridge over that region. In an observational study of summer precipitation in New Mexico and antecedent snow cover, Gutzler and Preston (1997) proposed that spring snow extent across the west-central U.S. acts to enhance or suppress the NAM circulation. Excessive snow leads to deficient summer rain, and deficient snow leads to abundant rain. In agreement with this hypothesis, Higgins et al. (1998) noted wet (dry) monsoons in Arizona-New Mexico tend to follow winters with wet (dry) conditions in the Pacific Northwest and dry (wet) conditions in the Southwest.

In this study, the original hypothesis of Gurshunov and Barnett (1998) is extended to the summer season. We propose that the combination of ENSO and NPO govern interannual variability of the NAM, as determined by monsoon ridge position. The NAM should show a strong relationship to Pacific SSTs, since it is the dominant summer circulation feature in the western U.S. The most coherent relationships between the NAM and Pacific SSTAs should occur when El Niño (La Niña) corresponds with high

(low) NPO phase. The datasets and methodology are discussed in sections 2 and 3. The results of an updated reanalysis NAM climatology of 500-mb geopotential height and atmospheric moisture for the summer season are shown in section 4. Interannual variability of the reanalysis variables and a precipitation index are related to Pacific SSTs in sections 5 and 6. Lagged relationships with Pacific SSTs are evaluated in section 7. A discussion and summary are presented in sections 8 and 9.

II. DESCRIPTION OF DATA

The updated NCEP/NCAR Daily Reanalysis is used to evaluate atmospheric circulation and moisture in the western U.S. The reanalysis assimilation system is a modified version of the Medium Range Forecast (MRF) spectral model with T62 resolution and 28 sigma levels. The NCEP/NCAR Reanalysis incorporates the widest possible array of data sources with advanced quality control and monitoring systems (Kalnay et al. 1995). The study of interannual climate variability is an intended use of long term reanalyses and the NCEP/NCAR Reanalysis has already been used for this purpose in previous work on the NAM (e.g. Higgins et al. 1998; Higgins et al. 1999; Higgins and Shi 2000). In this study we utilize the reanalysis specific humidity (q), surface pressure (p_s), and winds (v) for sigma levels 28-14 (below approximately 400-mb) and the 500-mb geopotential height (Φ_{500}). These reanalysis variables are more reliable, as compared to model parameterized variables like evaporation or precipitation, because they are directly influenced by the original radiosonde observations (Kalnay et al. 1995). Four times daily data (0Z, 6Z, 12Z, and 18Z) were obtained from the NCAR archives for the months May through September from 1948-98.

The Cooperative Summary of the Day (Coop) data, from the National Climate Data Center, has surface observations for all past and present cooperative sites throughout the United States. Daily precipitation is recorded as the precipitation reading 24 hours ending at the time of observation, read to hundredths of an inch. Trace amounts of precipitation are recorded. Missing precipitation is also recorded or, at some stations,

entire months are absent from the record. Daily Coop precipitation data from 1950-95 were obtained for 340 Great Plains stations (97-105° W, 37-45° N) and 231 Southwest stations (106-116° W, 31-39° N). The precipitation regions are shown in Fig. 1.

The Comprehensive Ocean Atmosphere Dataset (COADS) contains monthly average SST on a 2° latitude by 2° longitude grid from 1854-1997. SST observations are from ship reports and other in situ platforms. A quality control procedure eliminates outlying observations if they fall outside a prescribed number of standard deviations about the smoothed median at a specific location (Slutz et al. 1985). The normalized monthly SSTA from 1950-97 were computed for two regions of the North Pacific, the Central North Pacific or CNP (177° E-164° W, 26-36°N) and the Eastern North Pacific or ENP (125-150° W, 35-50° N). These Pacific regions correspond roughly to a SST dipole associated with the NPO and are correlated ($r^2 > 0.25$) with summer precipitation in the Great Plains (Ting and Wang 1997). The traditional Niño 3 normalized SSTA index to is used define ENSO. The Niño indices are readily accessible from the Climate Prediction Center. The Pacific SST regions are shown in Fig. 2.

III. ANALYSIS METHODS

Though precipitation is the principal variable of concern, the standard precipitation-based approaches may not be best suited to investigate NAM interannual variability. Summer precipitation is statistically ill-behaved. Its spatial distribution is more variable than winter precipitation because thunderstorms are forced by the large-scale dynamic and the local thermodynamic conditions. At point measuring locations, precipitation is not a normally distributed quantity and large rainfall events account for most precipitation variability in summer (e.g. Cowie and McKee 1986). Gridded precipitation products may smooth out maxima or be influenced by a reanalysis model parameterization, though the quality and length of these data have dramatically improved in recent years. The specific regions and analysis techniques used differ in every study, so there is no universally agreed set of dry and wet summers in a given region. Most important, the relationship of NAM precipitation to circulation and SSTs may change in time and space through the summer season. Monthly or seasonal averages are of insufficient time resolution to resolve the evolution. Daily data are necessary.

The daily integrated moisture flux (MF) and integrated moisture flux convergence (MFC) are better suited to investigate interannual variability of atmospheric moisture over a large region. At locations throughout the western U.S., the statistical distribution of MFC for each day is near normal in the summer season (not shown). The contribution of the large scale moisture transport to precipitation is isolated apart from local evaporation and transpiration. MF and MFC for each analysis time are computed from reanalysis winds (v) and specific humidity (q) on sigma surfaces. These variables are

directly related to evaporation (E) and precipitation (P) through the water balance equation (Trenberth and Guillemot 1995; Schmitz and Mullen 1996; Higgins et al. 1997a)

$$MF = \frac{p_s}{g} \int_{\sigma_{14}}^{\sigma_{28}} (q\bar{v}) d\sigma \tag{1}$$

$$MFC = P - E = -\frac{p_s}{g} \int_{\sigma_{14}}^{\sigma_{28}} \nabla \bullet (q\bar{v}) d\sigma \tag{2}$$

The version of the water balance equation used here for MFC omits local storage of water vapor, surface runoff, and ground storage. MFC for sigma levels 28-14 is computed by a step-wise integration procedure. Since the amount of water vapor at 400-mb is two orders of magnitude less than at the surface, transport of water vapor at upper levels (less than sigma level 14) is assumed negligible (e.g. Higgins et al. 1997b).

Five day running averages (μ) and standard deviations (σ) of the reanalysis MF, MFC, and Φ_{500} are constructed for each from May through September. Each of the four daily reanalysis times is considered separately. These fields yield an updated fifty-year reanalysis climatology of the height and moisture fields of the NAM that can be compared with similar, more comprehensive NAM climatologies using shorter lengths of record.

In the same manner as the precipitation studies, the reanalysis variables (χ) of MF, MFC, and Φ_{500} are converted to Z-scores (Z_χ) daily for the four reanalysis times. A spatially varying Z-score is defined for each time as:

$$Z_{\chi(t)} = \frac{\chi_{(t)} - \mu_{\chi(t)}}{\sigma_{\chi(t)}} \tag{3}$$

A time-varying correlation approach is used to relate Pacific SSTs, atmospheric circulation, and atmospheric moisture transport through the course of the summer season. For each reanalysis time, the thirty day average Z-score of the reanalysis variable centered on the date ($\overline{Z}_{\chi(t)}$) is correlated with time coincident values of three Pacific SSTA indices: the standard Niño 3, a North Pacific index, and a North American Monsoon index which combines the previous two. $\overline{Z}_{\chi(t)}$ isolates interannual to interdecadal climate variability by eliminating the diurnal, seasonal, and intraseasonal variability from the data. The NP index (NP) is:

$$NP = ENP - CNP \tag{4}$$

The North American Monsoon Index (M) is:

$$M = Niño\ 3 + ENP - CNP \tag{5}$$

This new simple M index is proposed as a way to relate the combination of temporal variability of ENSO and NPO. High (low) M corresponds with El Niño (La Niña) and high (low) NPO. The M index weights the influence of the North Pacific more than

tropical Pacific SSTs, reflecting the magnitude of correlation between Pacific SSTs and Great Plains summer precipitation found by Ting and Wang (1997). The relative contribution of tropical and North Pacific SSTs to the explained variance of M is evaluated by comparison of the correlation analyses from the first two Pacific SST indices. The same analyses were also done with one to four months lag in Pacific SSTs to evaluate the potential for seasonal predictability and the dependence of late spring Pacific conditions on the NAM. With the same time-evolving approach, the fifteen highest and lowest index years are composited and statistically significant differences are assessed in reanalysis variable Z-scores through the summer using a two-tailed student's t-test.

To evaluate the relationship of Coop precipitation data to Pacific SSTs, we introduce regional time evolving precipitation indices (PR) for the Great Plains and Southwest. At an individual station, for each day a thirty-day precipitation total is computed centered about the date. A missing thirty day total for the station is recorded if there are more than five missing days in the record. For each date the years are ordered highest to lowest according to the precipitation totals. The station precipitation total is considered above (below) average on that date if a given year ranks in the top (bottom) twenty years. The number of stations in the region (S) recording an above average (S_{wet}) or below average (S_{dry}) precipitation total are tallied for each date. The regional precipitation index is then

$$PR(t) = \frac{S_{wet}(t) - S_{dry}(t)}{S} \tag{5}$$

As with the Z-scores, the regional precipitation indices for the Great Plains and Southwest are correlated with the Pacific SST indices throughout the entire summer.

Considering summer precipitation in such a way has several advantages. As with the average Z-score correlation analyses for reanalysis variables, we consider a time-evolving relationship between Pacific SSTs and precipitation. The actual station precipitation totals, the accumulation of small-scale thunderstorm events, are less important than whether it was generally wet or dry over the area in the thirty-day period. The precipitation indices contain a large sampling of stations within each area, so any trends are likely to mirror those in MFC and reflect real large-scale climate variability.

IV. UPDATES TO EXISTING NAM REANALYSIS CLIMATOLOGIES

More comprehensive NAM climatologies using both the ECMWF and NCEP-NCAR reanalyses have been done by Schmitz and Mullen (1996) and Higgins et al. (1997b), respectively. The time series of daily average Φ_{500}, MF, and MFC we obtain here using the complete fifty-year record are consistent with this previous work. Here we show the *integrated* quantities of MF and MFC only, which are strongly influenced by conditions at the surface and low levels. To simplify our discussion, the evolution of the NAM is broken down into four averaged periods: pre-monsoon (15 May - 15 June), monsoon onset (16 June - 15 July), monsoon peak (16 July - 15 August), and monsoon end (16 August - 15 September).

The upper level monsoon ridge (Fig. 3) is principal control on interseasonal variability of MF and MFC. The ridge appears to be a westward extension of the Bermuda high, though continental heating is its physical mechanism of generation (Bryson and Lowry, 1955). The maximum northward extent of the monsoon ridge, or monsoon maximum, occurs in late July. At this time monsoon ridge is centered over the Four Corners region of the U.S. (Fig. 3c). The zonal component of MF (Fig. 4) shows that easterly moisture flux begins over the Gulf of Mexico in May, then advances north and westward into Mexico and the Southwest U.S. The deep easterly MF through Mexico at monsoon maximum suggests that the Gulf of Mexico, and not the Eastern Pacific, is the dominant contributor to the time-averaged moisture transport. The

monsoon ridge and easterly moisture flux gradually retreat in August and September as the mid-latitude westerly flow resumes.

The meridional component of MF (Fig. 5) shows the influence of the two low level jets, separated by a MF minimum over the Sierra Madre Occidental, eastern Arizona, and western New Mexico. The Great Plains LLJ extends from southern Texas northward to the Dakotas. This jet has its maximum spatial coverage and intensity in the Great Plains from May through early July corresponding with the time of most frequent and severe thunderstorms there (e.g. Higgins et al. 1997a). At monsoon onset the daily average MF exceeds 175 kg m s^{-1} in southern Texas near the Gulf of Mexico. The jet becomes less intense in the Great Plains from monsoon onset and is weakest at monsoon maximum, though it is still a dominant factor in summer rainfall. The meridional MF in the Southwest U.S. reflects the Baja LLJ. Though approximately four times weaker than the Great Plains LLJ, its time evolution is opposite. The time of maximum intensity and spatial coverage for the Baja LLJ is from monsoon onset through monsoon peak. The Baja LLJ appears to be strongest in the Colorado River Valley and originate in the northern Gulf of California. However, the NCEP/NCAR Reanalysis cannot resolve the structure of the jet within the Gulf of California itself, where the jet is observed to be a maximum (Douglas 1995). This analysis supports the assertion that the Gulf of Mexico and the Gulf of California are separate and distinct moisture sources for the NAM.

There is significant diurnal and seasonal variability in MFC. The seasonal and diurnal cycle of the Great Plains low level jet, MFC, and precipitation are discussed at length by Higgins et al. (1997a). The diurnal cycle of MFC (Fig. 6) reflects the evolution of summer thunderstorms, which initiate over mountains during the day, then intensify

and move towards lowland regions in the evening and nighttime. The 0Z component of the average daily MFC, which dominates the daily average over the western U.S. and Mexico, is the largest in magnitude. High values over the Rocky Mountains (9 mm day^{-1}) the Sierra Madre Occidental in Mexico (15 mm day^{-1}) reflect the strong convection there. The MFC maxima becomes weaker and moves to the Great Plains at night (6Z) when the Great Plains LLJ and thunderstorms are most active. From observational studies, a similar diurnal cycle exists in the Southwest U.S., in particular southwest Arizona (Adams and Comerie 1997). However, it is not well shown in Fig. 6 because the reanalysis resolution is too coarse to capture the sharp contrasts in topography from the Mogollon Rim to the Colorado River Valley.

The domain-averaged summertime evolution of the MFC for the Great Plains and the Southwest is computed using the dominant daily component (Fig. 7). The behavior of MFC is consistent with the evolution of the monsoon ridge and MF. The evolution of atmospheric moisture in Southwest is opposite of the Great Plains. In the Southwest (Great Plains) there is a late spring pre-monsoon dry (wet) period from May through mid-June. Monsoon onset is characterized by a rapid increase (decrease) in MFC, from approximately -1 (3.5) in mid-June to 0.5 (2) mm day^{-1} in mid-July. MFC increases to near 1 mm day^{-1} at monsoon maximum in late July. Values gradually decline (increase) into August and September as the monsoon ridge dissipates. The evolution of MFC through the summer in both regions is approximately the same as the seasonal precipitation (e.g. Higgins et al. 1997b, Barlow et al. 1998). This suggests MFC dominated by the large-scale circulation, in addition to local evaporation and transpiration, is probably an important factor in regional precipitation.

It should be noted that even at the time of minimum MFC in the Plains, values are still positive and thunderstorms typically occur. By contrast, usually little, if any, rainfall is received in the Southwest in the pre-monsoon period, where MFC is negative, on average. The onset date of the monsoon could be defined as the time when the dominant daily component of the MFC becomes positive in the Southwest. Using this definition, the monsoon onset date for the Southwest region is between 7 July and 14 July. This onset date is close to that obtained by Higgins et al. (1997a) using a high-resolution precipitation dataset over a smaller area within our Southwest region. However, the same reasoning does not apply when determining the monsoon end date. Average MFC becomes negative again after about 13 August, but monsoon rainfall typically persists for several weeks later into September. In the later part of the monsoon, local evaporation and transpiration may become a more important source of atmospheric moisture.

The standard deviation of MFC and Φ_{500} are fairly constant through the summer (Fig. 8) over the U.S. Geopotential heights and MFC are less variable in the western U.S. because of the influence of the monsoon ridge. The highest variability in MFC occurs near the Great Lakes region. Synoptic scale eddies associated with the polar front are the likely the dominant forcing mechanism for summer rainfall in that part of the U.S. MFC is least variable in the Southwest, where there is little atmospheric moisture, though the variability increases after monsoon onset. MFC variability increases sharply from west to east across the Great Plains, corresponding with a sharp increase in atmospheric moisture from the base of the Rocky Mountains to the Mississippi River Valley.

V. CORRELATION ANALYSES WITH THE M INDEX

A. Time series of Pacific SST Indices

The average summer Pacific SST indices for 1950-97 are shown in Fig. 9. The fifteen highest and lowest M index summers used for the two tailed student's t-test are indicated. We note, as in Mantua et al. (1997), that the NP and Niño 3 indices which compose the M index are not independent of each other. Niño 3 is most related to the NP index in spring and early summer, with an average correlation of 0.36 in the period March through July. Near zero values of the M index arise when Pacific SSTs are near average, such as 1959, or when strong tropical and North Pacific SSTs occur in destructive ENSO-NPO combinations, such 1976 and 1983. In the Great Plains, long-term variation in the M index seems to correspond with sustained dry (low M) or wet periods (high M). Using the standardized precipitation index (SPI) in Colorado, McKee et al. (1999) note the wet periods since 1950 as 1957-59, 1965-75, and 1979-96, and the dry periods as 1951-57, 1963-65, and 1975-78. An opposite relationship may exist in Arizona, which experienced wet summers in the mid-1950s coincident with frequent monsoon-related flash flood events (Carleton et al. 1990; Hirshboeck 1999). The following time-coincident correlation analysis with the M index is presented as 15 day snapshorts starting at Julian day 140 (20 May) through Julian day 245 (2 September). These dates capture all four periods of NAM evolution.

B. Upper level Circulation

There is a time evolution of correlation patterns between the M index and $\overline{Z}_{\Phi_{500}(t)}$ (Fig. 10). Pacific SSTAs are related to a coherent sequence of three atmospheric teleconnection patterns across the Pacific Ocean and North America during the course of the summer season. The North Pacific, Pacific Transition, and Pacific North America patterns are associated with the M index during the periods of pre-monsoon, monsoon onset, and late monsoon, respectively.

In the late spring pre-monsoon period (days 140 and 155), the M index is correlated with a positive phase of the North Pacific pattern, with height deviations in the western and central North Pacific ($r = -0.4$) and over southern Alaska ($r = 0.5$). The positive (negative) phase of the North Pacific pattern, a preferred El Niño (La Niña) response during the spring, is associated with a southward (northward) shift of the jet stream across the North Pacific (Bell and Jonowiak 1995). The spring storm track is directed toward southern California and the Southwest (Pacific Northwest). Though the positive (negative) phase of the North Pacific pattern in winter and spring brings above (below) average precipitation in the Southwest, it precedes dry (wet) monsoons (Higgins and Shi 2000).

The most statistically significant relationship between the M index and the upper level circulation is at monsoon onset in late June and early July, *not* monsoon peak in late July. At onset the M index is correlated with the negative phase of the Pacific Transition pattern (PT), which occurred in association with the Flood of 1993 in the Midwest U.S. (Bell and Jonowiak 1995). PT appears exclusively in summer and is distinct from the

ENSO-associated winter teleconnection patterns. The negative and positive phases of PT pattern match the monsoon ridge configurations described by Carleton et al. (1990) that govern upper level moisture transport and the onset date. A stronger than average upper level trough (M high) or ridge (M low) is centered in the northern Rocky Mountains and western Great Plains. The strongest negative correlation with $\overline{Z}_{\Phi_{500}(t)}$ in North America ($r = -0.6$, day 185) during the entire summer, significant at the 99% level, is centered over the northern Great Plains in late June to early July. Like the winter Pacific North America pattern, PT is part of a coherent series of height deviations from average that extend across the Pacific, with centers of action in the tropical Pacific near 160° E, 25° N ($r = -0.4$), central North Pacific in the CNP region ($r = -0.3$ to -0.4) and the Gulf of Alaska near the ENP region ($r = 0.4$). In late July and August (day 200 onward), the correlation between the M index and $\overline{Z}_{\Phi_{500}(t)}$ becomes statistically insignificant. The monsoon peak and end periods appear to be a time of transition to an early fall relationship with the Pacific North America pattern which develops in late August and September.

C. Atmospheric moisture

The correlation of $\overline{Z}_{MFC(t)}$ with the M index is controlled by the PT response (Fig. 11). The inverse relationship between atmospheric moisture in the Southwest and Great Plains exists interannually as well as seasonally. In the May through mid-June pre-monsoon period, there is a positive correlation ($r = 0.4$, days 140 and 155) in the southern Great Plains states of Texas and Oklahoma. There is no statistically significant

relationship in the Southwest at this time. When the position of the monsoon ridge is most related to the M index at monsoon onset, MFC is favored either in the Great Plains or Southwest. An area of negative correlation with $\overline{Z}_{MFC(t)}$ appears southern Arizona and western New Mexico (r = -0.4, days 170-185), significant at the 95% level. The area of positive correlation shifts northward into central Great Plains and the Midwest, increasing in spatial coverage and magnitude (r = 0.4 to 0.6, days 170-185), significant at the 99% level in Colorado, Kansas, Nebraska, Iowa, and Missouri. The maximum correlation of the M index with $\overline{Z}_{MFC(t)}$ through the onset period follows the climatological northward progression of the monsoon, reaching South Dakota and Utah by mid-July. Proceeding into late July and August, the correlation decays with time. By the time of monsoon maximum, as with $\overline{Z}_{\Phi_{500}(t)}$, the statistical relationship between the M index and $\overline{Z}_{MFC(t)}$ is virtually insignificant across the western U.S. and remains so for the rest of the summer.

The correlation of $\overline{Z}_{MF(t)}$ with the M index, presented as a vector, parallels the evolution of cyclonic (high M) or anticyclonic (low M) contributions to the circulation centered in the northern Great Plains at monsoon onset (Fig. 12). Decomposing the MF into low (sigma levels 22-28) and mid levels (sigma levels 14-22), the correlation with $\overline{Z}_{MF(t)}$ at mid-levels is nearly identical to the integrated quantity (not shown). The M index has the strongest correlation with $\overline{Z}_{MF(t)}$ across the Southwest and the southern Great Plains, particularly in New Mexico (r= 0.65, day 185). Though Mo et al.(1997) showed that wet summer periods in the central U.S. are associated with a stronger meridional moisture flux, it is the zonal component of the flux which varies most with the M index. This result is consistent with the relationship of the M index to the large-scale

circulation pattern. Upper level moisture flux is controlled by the circulation anomaly in the northern Great Plains, favoring deviations from the average which are westerly (high M) or easterly (low M) to the south and west.

Correlation with low-level $\overline{Z}_{MF(t)}$ is weaker and generally of the same sign, though not statistically significant in the locations of the two low level jets (not shown). In spite of the weak statistical relationship with the M index, there are convincing physical arguments that relate the low level jets to Pacific SSTs. The presence of a surface ridge or trough in the Great Plains associated with the PT pattern modulates the strength of the Great Plains LLJ, directing low level moisture into eastern Mexico or the central U.S. (Mo et al. 1997). The SST gradient between the Gulf of California and East Pacific would be enhanced (diminished) in La Niña (El Niño) conditions, strengthening (weakening) the Gulf surges associated with the Baja LLJ (Carleton et al. 1990). The Baja LLJ would be stronger (weaker) in low (high) M years and oriented more from the southeast. Such an orientation would place the jet over the axis of the Gulf of California, favorable to carry the most amount of low level moisture into the Southwest (Douglas 1995). A more detailed reanalysis over North America, long-term observational studies of both low level jets, and associated regional atmospheric modeling are necessary to validate these hypotheses.

The high and low M index composite summertime evolution of MFC was constructed (Fig. 13) using the fifteen highest and lowest summer average M index years shown in Fig. 9. These fifteen-year averages are comparable to the fifty year MFC climatology in Fig. 7. The greatest differences in MFC between high and low M index

years and climatology in the Great Plains and Southwest are at monsoon onset. Differences in MFC evolution in the Southwest begin in mid-June. Using the definition described earlier, there is a difference of about ten days in onset dates between high (16 July) and low M (5-6 July) years in the Southwest. These onset dates are slightly outside the bounds of the fifty-year climatology. Differences in Great Plains MFC become apparent by the beginning of June. MFC increases (decreases) in the Great Plains after this time in high (low) M index years. The climatological decrease in MFC which occurs near the beginning of July is delayed until early to mid July in high M index years. The absolute percentage difference in MFC from climatology for high and low M index years is much higher in the Great Plains (50-100%) than the Southwest (5-10%), where moisture is less variable, on average. The evolution of MFC abruptly reverts to climatology after late July, when the statistical relationships between MFC and the M index become insignificant.

Central and southern Mexico are not focus of this study, but this area deserves mention because NAM precipitation is most pronounced there. Statistically significant relationships have been found to exist between summer precipitation and tropical Pacific SSTs in this region (Higgins et al. 1999). There is a slight negative relationship of $\overline{Z}_{MFC(t)}$ to the M index, and Niño 3, in late June and July, but it is not as statistically significant nor persistent as the relationship in the Southwest U.S. (not shown in Fig. 11). Long term reanalysis atmospheric moisture may be worse over Mexico because of the paucity of continuous rawinsonde records. Also, the interannual variability of the NAM in Mexico is probably less sensitive to the mid-latitude atmospheric teleconnection patterns

associated with remote Pacific SSTs. Summer precipitation in Mexico is more likely tied to SSTs in the adjacent East Pacific, which in turn vary with ENSO. Colder (warmer) SSTs along the western Mexican coast would enhance (diminish) the ocean-land temperature gradient, hence the strength of the monsoon (Higgins et al. 1999). However, east Pacific tropical systems are more frequent and intense in El Niño years, which would tend to disrupt this relationship (Reyes and Mejìa-Trejo, 1991; Kimberlain and Landsea, 2000). Mexican rainfall may also be influenced by factors independent of Pacific SSTs not considered here, such as the quasi-biennial oscillation (A. Douglas, personal communication). Because of the difference in climatological evolution and possible difference of controls on interannual variability, the NAM in Mexico should be treated separately from the NAM in the U.S.

D. Precipitation Indices

The behavior of the correlation of Great Plains and Southwest precipitation indices with the M index shows some difference from the correlation with $\overline{Z}_{MFC(t)}$, but results are broadly consistent (Fig. 14). The greatest discrepancy is during the premonsoon period in the Southwest, when the precipitation index shows a strong positive correlation with the M index ($r > 0.5$). The positive relationship in the spring reflects the influence of the North Pacific pattern on the winter and spring storm track into the Southwest U.S. However, as the PT relationship emerges and the monsoon ridge becomes the dominant control on precipitation in mid June the correlation between the Great Plains and Southwest begins to diverge. The maximum correlation with the M

index occurs near monsoon onset, 29 June (Julian day 180) in the Great Plains ($r = 0.64$) and 9 July (Julian day 190) in the Southwest ($r = -0.37$). Precipitation between the Great Plains and Southwest is inversely related until the end of July. Beyond late July the correlation with M in the Southwest is weakly positive, but not statistically significant. A secondary maxima in correlation appears in the Great Plains in August which does not appear in MFC, possibly due to moisture recycling by local evaporation and transpiration. The precipitation indices, however, are able to capture the same time evolution of the NAM relationship to the M index revealed in MFC, particularly at monsoon onset. They confirm that a conclusive link exists between reanalysis MFC and point source station precipitation data considered over broad regions, at least in the U.S.

VI. COMPARISON OF M INDEX TO NIÑO 3 AND NP INDICES

Now that a statistically significant relationship between the M index and atmospheric circulation, atmospheric moisture, and precipitation has been established, we compare the time-coincident correlation results with those using the Niño 3 and NP indices. The sign of the correlation associated with Niño 3 and NP in locations of high explained variance is nearly identical to that of the M index. Only the average of the explained variance of $\overline{Z}_{\chi(t)}$ in the monsoon onset period is considered since the relationship of the summertime circulation and moisture to Pacific SSTs is strongest at this time.

The explained variance (r^2) of $\overline{Z}_{\Phi_{500}(t)}$ show tropical and North Pacific SSTs are associated with two distinct circulation responses over the eastern Pacific and North America in early summer (Fig. 15). The tropical Pacific response (Fig. 15a) has centers of action in the central North Pacific near 180°, 40° N and northern Rocky Mountains of the U.S. The North Pacific response (Fig. 15 b) has centers of action in the central North Pacific just northeast of the Hawaiian islands, southeast Gulf of Alaska, and the upper Midwest and northern Great Plains. Over North America, the North Pacific response is approximately twice as large as the tropical Pacific response at monsoon onset. Niño 3, not surprisingly, explains a greater amount of variance toward the equatorial Pacific. The M index (Fig. 15c) explains the variability of $\overline{Z}_{\Phi_{500}(t)}$ in the same locations as the NP and Niño 3 indices. Maxima in explained variance over the Pacific are reduced at the centers

of action, but are still present and statistically significant. The highest magnitude of explained variance, over the northern U.S., is preserved and shifts into the northern Great Plains ($r^2 \cong 0.25$). These tropical and North Pacific associated circulation responses together contribute toward the relationship of the M index to the PT response. A low (high) NP index is related to a northeast (southwest) displacement of the monsoon ridge from its climatological position. A low (high) Niño 3 is related to a north (south) displacement of the ridge.

The largest improvement in explained variance by the M index over Niño 3 and NP indices is for $\overline{Z}_{MF(t)}$ (Fig. 16). In Fig. 16, the orientation of the vectors reflect the circulation in the northern Rocky Mountains associated with Niño 3 (Fig. 16a) and the circulation anomaly in the upper Midwest associated with the NP index (Fig. 16b). The vectors in Fig. 16b also indicate the tendency for a trough or ridge off the west coast of North America. As with the M index, most of the explained variability is in the zonal component of $\overline{Z}_{MF(t)}$ and the mid-level component is the dominant factor. The tropical and North Pacific-related circulation anomalies in the northern U.S. *together* explain the most variability in mid-level MF over the Southwest U.S. and northwest Mexico. The NP index explains the most variance in over the Southwest U.S., particularly east of the continental divide in New Mexico. Niño 3 explains more variance in northwest Mexico and near the Gulf of California. The M index explains the most variance of $\overline{Z}_{MF(t)}$ over the Southwest (Fig. 16c), with increases in New Mexico by approximately 20% over the Niño 3 index (Fig 17a) and in northwest Mexico by approximately 5-10% over the NP index (Fig. 17b).

The spatial relationship of tropical and North Pacific SSTs to Great Plains and Midwest $\overline{Z}_{MFC(t)}$ (Fig. 18) and precipitation indices is agreement with the precipitation modes in central U.S. precipitation found by Ting and Wang (1997). The NP index is most related to $\overline{Z}_{MF(t)}$ in regions where precipitation is dependent on the position of the monsoon ridge: the central Great Plains, eastern Arizona, western New Mexico and the Midwest, namely eastern Nebraska and Iowa (Fig.18b). The relationship of Niño 3 to MFC is substantially weaker (Fig. 18a), but maxima in explained variance occur in the northern Great Plains and Midwest and the area of southwest Arizona and northwest Mexico, especially near the Gulf of California. As with $\overline{Z}_{\Phi_{500}(t)}$, the M index captures all the maxima in explained variance of both indices. Where NP and Niño 3 indices both explain variance in MFC, such as in the Midwest and near the Gulf of California, there are slight improvements with the M index. Using the precipitation indices, we found that the maximum correlation in the Great Plains using the NP index is virtually the same as with the M index. In the Southwest the M index improves the correlation by approximately 0.07 over either the Niño 3 or NP index.

The M index accounts for a dual relationship of tropical and North Pacific SSTs to NAM circulation and moisture sources. In the Midwest, both the tropical and North Pacific SSTs are related to variability in early summer rainfall. In the Great Plains, however, only North Pacific SSTs are important. An upper level trough or ridge over the upper Midwest associated with the North Pacific circulation response is the determining factor of Great Plains LLJ strength and thunderstorm activity downwind of the jet. The mid-level moisture flux has a spatially varying relationship with NP and Niño 3 across

the Southwest and northwest Mexico. The Baja LLJ moisture, related to east Pacific SSTs, is most important for thunderstorms in the Colorado River Valley and southwestern Arizona. The mid-level Gulf of Mexico moisture, associated more with the NP circulation response, becomes increasingly important for monsoon thunderstorms farther north and east from the Gulf of California, in areas such as eastern Arizona and western New Mexico.

VII. TIME LAGGED RELATIONSHIPS WITH PACIFIC SST INDICES

The simultaneous correlation analyses presented in sections 4 and 5 were repeated with the Pacific SST indices lagged from one to four months. Only the variables of $\overline{Z}_{\Phi_{500}(t)}$ and $\overline{Z}_{MFC(t)}$ are considered for the period of monsoon onset. The relationship of Niño 3 with $\overline{Z}_{\Phi_{500}(t)}$ shows the tropical Pacific circulation response is strongest at simultaneous correlation and statistically significant at the 90% level up to a two month lag (Fig. 19). Using early spring Niño 3 conditions at three and four month lag the spatial structure of the response is preserved, but not statistically significant. Though the M and NP indices improve over Niño 3 for simultaneous correlation, the North Pacific response becomes statistically insignificant at just a two month lag (Figs. 20 and 21). Spring North Pacific SSTs, at least in the regions used for the M and NP indices, have little relationship to summer atmospheric circulation anomalies. A similar result was obtained by Ting and Wang (1997) in a lag correlation of summer average 500-mb height with a North Pacific mode of SST related to precipitation variability in the central U.S. In regions where variability in MFC is explained by Niño 3, such as the upper Midwest and southwest Arizona, correlation is still statistically significant at the 90% level up to a two months lag using the Niño 3 index (not shown). Areas where MFC is related to the NP index, such as the central Great Plains, eastern Arizona, and western New Mexico, have no significant relationship to any of the Pacific SST indices beyond two month lag.

Higgins et al. (1999) showed that an association with tropical Pacific SSTs is important for the NAM. Prior to wet monsoons, cold SST anomalies appear in the

equatorial Pacific cold tongue near the dateline in winter and increase in amplitude during the spring. These changes in tropical Pacific SST are associated with a weakened, northward displaced ITCZ and suppressed local Hadley circulation. The opposite is true for dry monsoons. The coherence of summer circulation anomalies with antecedent spring Niño 3 suggests tropical Pacific SSTs may be a good NAM predictor, though the physical mechanisms relating the two need to be investigated.

The weak lag correlation using the M and NP indices may be an artifact of the regions used to define them. Other areas in the North Pacific, besides those used for the NP and M indices, may be more related to the NAM in the spring season. Since NAM interannual variability is related to the occurrence of the North Pacific pattern, the regions of SST associated with this winter and spring teleconnection should have a relationship to subsequent summer conditions. Higgins and Shi (2000) demonstrated that early onset monsoons in the Southwest are associated with warm SSTs in the subtropical North Pacific (near 170° W, 20° N) and cold SSTs in mid-latitude central North Pacific (180°, 40° N) during winter. This distribution of SSTs is consistent with a negative phase of the North Pacific pattern, with cold SSTs in the vicinity of large sensible and latent heat fluxes near the northward-displaced jet stream. Higgins and Shi also developed a winter North Pacific SST index, similar in principle to the NP index in this study, and demonstrated its usefulness in predicting the monsoon onset date.

The North Pacific summer teleconnection may be indirectly related to ENSO. Coupled ocean-atmosphere general circulation model simulations suggest the North Pacific SST dipole develops as result of near time-coincident atmospheric forcing by

ENSO-related tropical convection (Lau and Nath 1994). The variations in North Pacific SSTs may then feedback to the summer atmospheric circulation over North America with a timescale of several weeks (Ting and Wang, 1997). The strength of the North Pacific SST dipole, by controlling the latitudinal temperature gradient, determines the strength and position of summer jet stream. If such a mechanism is at work, summer North Pacific SSTs captured by M and NP indices would probably not persist from the previous seasons.

VIII. DISCUSSION

The contrasting summers of 1993 and 1988 are examples of large departures from average summer climatology associated with high and low M index, respectively. The influences of remote Pacific SST and land surface forcing have been rigorously investigated in both years. In the Midwest Flood of 1993, a strong trough situated over the northern Rocky Mountains and northern Great Plains maintained westerly flow across all of the western U.S. in the summer. The jet stream and associated synoptic eddies were stronger than average and south of their mean climatological position. The Great Plains and Midwest, to the east of the trough and north of the jet stream, were favored for the development of thunderstorms in the form of mesoscale convective complexes (Bell and Jonowiak 1995; Mo et al. 1997; Trenberth and Guillemot 1996). Monsoon rainfall in the Southwest was below average because onset was delayed until early August, the latest onset on record since 1948 (Okabe 1995; Higgins and Shi 2000). By contrast, in the Drought of 1988, a monsoon ridge located over the Great Plains steered the jet stream north into Canada from late spring into early summer (Bell and Jonowiak 1995; Trenberth 1992). The Great Plains and Midwest, on the subsiding branch of the ridge, received little precipitation and temperatures were much above average. There was enhanced easterly flow on the southern side of the ridge. The monsoon began early in late June and summer rainfall was above average in the Southwest (Higgins and Shi 2000). Though this circulation pattern broke down in mid-July and rainfall returned to normal in the central U.S., the late summer rains were insufficient to break the hydrologic drought (Trenberth and Guillemot 1996).

Modeling studies of 1988 and 1993 suggest the distribution of tropical *and* mid-latitude Pacific SSTs, and associated diabatic heating patterns, produced a *time-coincident* PT teleconnection response. Trenberth and Branstator (1992) argued latitudinal variation in the ITCZ changed the distribution of tropical Pacific heating, in agreement with observations of the dry and wet monsoon years (e.g. Higgins et al. 1998). Using a linearized baroclinic model, they showed these heating patterns provide the sources and sinks for quasi-stationary Rossby waves that propagate into the extratropics. Liu et al. (1996) took a similar modeling approach with a stationary wave model linearized about the mean summer climate. However, they found the summertime circulation pattern over North America was relatively insensitive to diabatic heating in the tropical Pacific. The greater effect on the circulation over North America was from diabatic heating associated with an upper level trough or ridge off the west coast of the continent and vorticity forcing by transient eddies. Both tropical and North Pacific SST forcing are probably important in early summer, because each is associated with a *distinct* circulation response.

The other possibility is that the NAM evolution is determined by the amount of snow cover over the Southern Rocky Mountains (Gutzler and Preston, 1997). The snow cover would affect the surface energy budget of the Rocky Mountains and Colorado Plateau in late spring, and, hence, the evolution of the monsoon ridge. Such a mechanism has been demonstrated for the Asian monsoon (e.g. Meehl, 1994), but no corresponding model studies have been done for the NAM. We suspect, however, that tropical Pacific SST forcing is the dominant factor in the winter *and* summer climate of the Southwest U.S. The relationship between snowfall and NAM precipitation is likely observed as a

coincidence of the changes in large-scale teleconnection patterns associated with ENSO-NPO and precipitation in the Southwest between winter and summer. A year with sustained El Niño, high NPO conditions, for example, would be associated with a positive phase of the North Pacific pattern in spring and a negative phase of the PT pattern in summer. The late winter and spring period would have more frequent and intense synoptic-scale systems directed toward the Southwest that would build a high snow pack in the Southern Rocky Mountains. However, NAM precipitation would be below average in summer, especially at monsoon onset. The reverse would be true with La Niña, low NPO.

If the evolution of the NAM in the U.S. is primarily driven by remote Pacific SST forcing in the early part of the monsoon, what happens during pre-monsoon and late monsoon "transition" periods in ENSO-NPO teleconnection relationships? We speculate at these times soil moisture, vegetation, and snow cover, may become more important for the large-scale circulation. In 1988 and 1993, antecedent soil moisture influenced surface sensible and latent heat fluxes. These surface energy fluxes may have provided positive or negative feedback to the drought or flood conditions (Giorgi et al. 1996; Trenberth and Guillemot 1996). Land surface feedback processes may be an equally important control on summer climate in the western U.S. Future investigation of the NAM should explore the physical linkages between remote Pacific SST forcing, land surface processes, and NAM evolution. Regional atmospheric models are well suited to such a task.

The fact that ENSO-NPO relationships with precipitation in the Southwest dramatically change through the season is a complicating factor in forecasting long-term drought or wet conditions in that region. The Great Plains is the region most sensitive to

interannual variability of the NAM. From the record of historically wet and dry periods found by McKee et. al. (1999), long-term climate variability there mirrors long-term variability in ENSO-NPO. Weather conditions in early summer must be a critical factor in determining the annual soil moisture surplus or deficit. Though there have been very dry summers like 1988 or 1983, the Great Plains have not experienced a long-term multiyear drought in the past two decades, corresponding with a period of sustained El Niño-high NPO conditions. The Great Plains could expect a greater frequency of long-term drought should these conditions change in the future.

IX. SUMMARY

In this study, a NAM reanalysis climatology of 500-mb geopotential height, integrated moisture flux, and integrated moisture flux convergence was computed using the fifty year NCEP-NCAR daily reanalysis. A time-varying correlation approach was used to relate daily deviations from the climatology to three Pacific SST indices which capture the variability of ENSO, NPO, and the combination of the two. New time-evolving precipitation indices, of Southwest and Great Plains stations, were also related to these Pacific SST indices.

The results of the updated reanalysis NAM climatology are consistent with previous, more extensive climatologies. The monsoon ridge and associated easterly moisture flux attain their maximum northward position by late July. The Great Plains and Baja LLJs, which supply low-level moisture from the Gulf of Mexico and Gulf of California sources, are maximum in late spring and mid-summer, respectively. There are diurnal and seasonal cycles in integrated moisture convergence. The diurnal cycle reflects the daily evolution of convective activity from the mountains in the morning to the lowlands at night. As the monsoon ridge develops during the monsoon onset period, there is a rapid increase (decrease) in atmospheric moisture and precipitation in the Southwest (Great Plains). This regime persists until the end of the monsoon in September.

Using the combined M index, Pacific SSTs are related to a sequence of teleconnection patterns over North America through the summer. The strongest relationship is at monsoon onset, when the PT pattern controls the large scale distribution

of moisture across the western U.S. (Fig. 22). High (low) M index years are characterized by a negative (positive) phase of this teleconnection pattern. A trough (ridge) is located over the northern Rocky Mountains and central Great Plains. Because the spring wet season is lengthened (shortened), early summer MFC and rainfall are above (below) average. In the Southwest, monsoon onset is late (early), and early summer MFC and rainfall are below (above) average. These relationships decay in the later part of the monsoon. It is the variability of mid-level moisture flux from the Gulf of Mexico which is most related to Pacific SSTs, but the Great Plains and Baja LLJs are likely related to Pacific SSTs in the same way.

Tropical and North Pacific SST variability are related to the deviation of the monsoon ridge from its climatological average position at monsoon onset. Tropical Pacific SSTs are related to the variation in ridge position to the north and south and North Pacific SSTs to variation in ridge position to the northeast and southwest. Using the combined M index, the largest departures in Φ_{500} are in the northern Rocky Mountains and northern Great Plains, consistent with the monsoon ridge configurations of Carleton et al. (1990) associated with interannual variability of the NAM precipitation in the Southwest. *Both* tropical and North Pacific circulation responses are related to MF, MFC, and precipitation in the western U.S. *to varying degrees depending on location*. In the Great Plains, North Pacific SSTs are the dominant factor, while in the Southwest tropical and North Pacific SSTs are equally important. The most coherent summer climate patterns over the entire western U.S. occur when Pacific SSTs are in a

substantially high or low M configuration, indicating that there is a constructive interference of ENSO and NPO in the summer as well as winter.

Though the M index is the better diagnostic for summer climate in the western U.S., it is not a good predictor. At one month lag, the relationships between the NP index and atmospheric circulation and moisture are statistically insignificant. The lack of coherence in correlation in the spring season may be due to the particular regions used to define the NP index. North Pacific SSTs may also be forced by time-coincident variations in tropical convection. However, statistically significant relationships with Niño 3 and 500-mb height exist up to three month lag. The Niño 3 index from mid-spring onward may be a good predictor of the atmospheric circulation pattern over North America at monsoon onset.

X. REFERENCES

Adams, D.K. and A.C. Comerie, 1997. The North American Monsoon. *Bull. Amer. Meteor. Soc.*, **78**, 2197-2213.

Anthes, R.A. and Y.H. Kuo, 1986. The Influence of Soil Moisture on Circulations over North America on Short Time Scales. *Namias Symposium, Scripps Institution of Oceanography Reference Series 86-17*, J.O. Roads, Ed., 132-147.

Barlow, M., S. Nigam, and E.H. Berbery, 1998. Evolution of the North American Monsoon System. *J. Climate*, **11**, 2238-2257.

Bell, G.D. and J.E. Janowiak, 1995. Atmospheric circulation associated with the Midwest floods of 1993. *Bull. Amer. Meteor. Soc.*, **76**, 681-695.

Brenner, I.S., 1974. A surge of maritime tropical air--Gulf of California to the southwestern United States. *Mon. Wea. Rev.*, **102**, 375-389.

Bryson, R.A. and W.P. Lowry, 1955. The synoptic climatology of the Arizona summer precipitation singularity. *Bull. Amer. Meteor. Soc.*, **36**, 329-339.

Bunkers, M.J., J.R. Miller, and A.T. DeGaetano, 1996. An examination of El-Niño-La Niña Related Precipitation Anomalies across the Northern Plains. *J. Climate*, **9**, 147-160.

Carleton, A.M., D.A. Carpenter, and P.J. Weser, 1990. Mechanisms of Interannual Variability of the Southwest United States Summer Rainfall Maximum. *J. Climate*, **3**, 999-1015.

Comerie, A.C. and E.C. Glenn, 1998. Principal components-based regionalization of precipitation regimes across the southwest United States and northern Mexico, with an application to monsoon precipitation variability. *Clim. Res.*, **10**, 201-215.

Cowie, J.R. and T.B. McKee, 1986. *Colorado Precipitation Event and Variability Analysis*. *Climatology Report 86-3*. Department of Atmospheric Science, Colorado State University. 102 pp.

Dirmeyer, P.A., 1994. Vegetation Stress as a Feedback Mechanism in Midlatitude Drought. *J. Climate*, **7**, 1463-1487.

Douglas, M.W., R.A. Maddox, K. Howard, and S. Reyes, 1993. The Mexican Monsoon. *J. Climate*, **6**, 1665-1677.

Douglas, M.W., 1995. The Summertime Low-Level Jet Over the Gulf of California. *Mon. Wea. Rev.*, **123**, 2334-2347.

Giorgi, F., L.O. Mearns, C. Shields, and L. Mayer, 1996. A regional model study of the importance of local versus remoste controls of the 1988 drought and 1993 flood over the central United States. *J. Climate*, **9**, 1150-1162.

Gurshunov, A. and T.B. Barnett, 1998. Interdecadal Modulation of ENSO Teleconnections. *Bull. Amer. Meteor. Soc.*, **79**, 2715-2775.

Gutzler, D.S. and J.W. Preston, 1997. Evidence for a relationship between spring snow cover in North American and summer rainfall in New Mexico. *Geophys. Res. Let.*, **24**, 2207-2210.

Hales, J.E., 1972. Surges of maritime tropical air northward over the Gulf of California. *Mon. Wea. Rev.*, **100**, 298-306.

Harrington, J.A., R.S. Cerveny, and R.C. Balling, 1992. Impact of the Southern Oscillation on the North American Monsoon. *Phys. Geog.*, **13**, 318-330.

Higgins, R.W., Y. Yao, E.S. Yarosh, J.E. Janowiak, and K.C. Mo, 1997a. Influence of the Great Plains Low-Level Jet on Summertime Precipitation and Moisture Transport over the Central United States. *J. Climate*, **10**, 481-507.

------, Y.Yao, and X.L. Wang, 1997b. Influence of the North American Monsoon System on the U.S. Summer Precipitation Regime. *J. Climate*, **10**, 2600-2622.

------, K.C. Mo, and Y. Yao, 1998. Interannual Variability of the U.S. Summer Precipitation Regime with Emphasis on the Southwestern Monsoon. *J. Climate*, **11**, 2582-2606.

------, Y. Chen, and A.V. Douglas, 1999. Interannual variability of the North American warm season precipitation regime. *J. Climate*, **12**, 653-680.

------ and W. Shi, 2000. Dominant Factors Responsible for Interannual Variability of the Summer Monsoon in the Southwestern United States. *J. Climate*, **13**, 759-775.

Hirschboeck, K.K., 1999. Implications for Climatological Forecasts of Hydrological Extremes. *Twenty-Fourth Climate Diagnositics and Prediction Workshop*, Tucson, Arizona.

Horel, J.D. and J.M. Wallace, 1981. Planetary-scale Atmospheric Phenomena Associated with the Southern Oscillation. *Mon. Wea. Rev.*, **109**, 813-829.

Kalnay, E., M. Kanamitsu, R. Kistler, W. Collins, D. Deaven, J. Derber, L. Gandin, S. Sara, G. White, J. Woollen, Y. Zhu, M. Chelliah, W. Ebisuzaki, W. Higgins, J. Janowiak, K.C. Mo, C. Ropelewski, J. Wang, A. Leetmaa, R. Reynolds, and

R. Jenne, 1995. The NCEP/NCAR reanalysis project. *Bull. Amer. Meteor. Soc.*, **77**, 437-471.

Kimberlain, T. and C. Landsea, 2000. A Climatology of East Pacific Tropical Cyclones: 1966-1997. *J. Climate*, submitted.

Lau, N.C. and M.J. Nath, 1996. The Role of the "Atmospheric Bridge" in Linking Tropical Pacific ENSO Events to Extratropical SST Anomalies. *J. Climate*, **9**, 2036-2057.

Liu, A.Z., M. Ting, and H. Wang, 1998. Maintenance of Circulation Anomalies during the 1988 Drought and 1993 Floods over the United States. *J. Atmos. Sci.*, **55**, 2810-2832.

Livezey, R.E. and K.C. Mo, 1987. Tropical-Extratropical Teleconnections during the Northern Hemisphere Winter. Part II: Relationships between Monthly Mean Northern Hemisphere Circulation Patterns and Proxies for Tropical Convection. *Mon. Wea. Rev.*, **115**, 3115-3132.

Mantua, N.J., S.R. Hare, U. Zhang, J.M. Wallace, and R.C. Francis, 1997. A Pacific interdecadal climate oscillation with impacts on salmon production. *Bull. Amer. Meteor. Soc.*, **78**, 1069-1079.

McKee, T.B., N.J. Doesken, and J. Kleist, 1999. *Historical Dry and Wet Periods in Colorado. Climatology Report 99-1, Part A: Technical Report*, Department of Atmospheric Science, Colorado State University, 121 pp.

Meehl, G.A., 1994. Influence of the land surface in the Asian summer monsoon: External conditions versus internal feedbacks. *J. Climate*, **7**, 1033-1049.

Minobe, S., 1997. A 50-70 year climatic oscillation over the North Pacific and North America. *Geophys. Res. Lett.*, **24**, 683-686.

Mo., K.C., J.N. Paegle, and R.W. Higgins, 1997. Atmospheric Processes Associated with Summer Floods and Droughts in the Central United States. *J. Climate*, **10**, 3028-3046.

Okabe, I.T., 1995. *The North American Monsoon*. Ph.D. dissertation, University of British Columbia, 146 pp.

Namias, J., 1960. Influences of abnormal surface heat sources and sinks on atmospheric behavior. *Proc. International Symposium on Numerical Weather Prediction in Tokyo, Meteor. Soc. Japan (published March 1962)*, 615-627.

Rasmussen, E.M., 1967. Atmospheric water vapor transport and the water balance of North America, Part I: Characteristics of the water vapor flux field. *Mon. Wea. Rev.*, **95**, 403-427.

Retian, C.H., 1957. The role of precipitable water in Arizona's summer rains. *Tech. Rep on the Meteorology and Climatology of Arid Regions 2*, The Institute of Atmospheric Physics, University of Arizona, Tucson, 19 pp.

Reyes, S. and A. Mejìa-Trejo, 1991. Tropical perturbations in the eastern Pacific and the precipitation field over north-western Mexico in relation to the ENSO phenomenon. *Int. J. Climatol.*, **11**, 515-528.

Ropelewski, C.F. and M.S. Halpert, 1986. North American Precipitation and Temperature Patterns Associated with the El Niño Southern Oscillation (ENSO). *Mon. Wea. Rev.*, **114**, 2352-2362.

Schmitz, J.T. and S. Mullen, 1996. Water vapor transport associated with the summertime North American Monsoon as depicted by ECMWF analyses, *J. Climate*, **9**, 1621-1634.

Slutz, R.J., S.J. Lubker, J.D. Hiscox, S.D. Woodruff, R.L. Jenne, D.H. Joseph, P.M. Stehrer, J.D. Elms, 1985. *Comprehensive Ocean Atmosphere Data Data Set; Release 1. NOAA Environmental Research Laboratories, Climate Research Program, Boulder, CO*, 268 pp.

Sud, Y.C., K.M. Lau, G.K. Walker and J.H. Kim, 1995. Understanding biosphere-precipitation relationships: Theory, model simulations, and logical inferences. *Mausam.*, **46**, 1-14.

Ting, M. and H. Wang, 1997. Summertime U.S. Precipitation Variability and Its Relation to Pacific Sea Surface Temperature. *J. Climate*, **10**, 1853-1873.

Trenberth, K.E. and G.W. Branstator, 1992. Issues in establishing causes of the 1988 drought over North America. *J. Climate*, **5**, 159-172.

------ and C.J. Guillemot 1995. Evaluation of the global atmospheric moisture budget at seen from analyses. *J. Climate*, **8**, 2255-2272.

------ and C.J. Guillemot, 1996. Physical Processes Involved in the 1988 Drought and 1993 Floods in North America. *J. Climate*, **9**, 1288-1298.

XI. LIST OF FIGURES

Figure 8. June-August average standard deviation of (a) 500-mb geopotential height (units: m) and (b) integrated moisture flux convergence (units: mm day^{-1}). Contour interval is 10 m in (a) and 1 mm day^{-1} in (b).

Figure 9: Average June-August values of (a) M index, (b) NP index, and (c) Niño 3 index from 1950-97. The fifteen highest and lowest years used in the student's t-test for time-coincident correlation are indicated.

Figure 10. Correlation (r) of time-coincident M index with $\overline{Z}_{\Phi_{500}(t)}$ from Julian Day 140 (20 May) through Julian Day 245 (2 Sep). Contour interval is 0.1 and absolute values less than 0.2 are not shown. Dark and light shaded regions indicate statistical significance at the 95% level by the two-tailed student's t-test.

Figure 11. Same as Fig. 10 for $\overline{Z}_{MFC(t)}$.

Figure 12. Same as Fig. 10 for $\overline{Z}_{MF(t)}$ except two-tailed student's t-test not shown. Vector length is 1.

Figure 13. Same as Fig. 7 for the fifteen composite high M index (solid) versus low M index (dashed) years.

Figure 14. Correlation (r) of time-coincident M index with regional precipitation indices for the Great Plains (solid) and Southwest (dashed), Julian Day 120 (1 May) through Julian Day 260 (30 September). Dates of highest correlation in the monsoon onset period are indicated.

Figure 15. Average percent explained variance (r^2) of $\overline{Z}_{\Phi_{500}(t)}$ in the monsoon onset period by time-coincident (a) Niño 3, (b) NP index, and (c) M index. Contour interval is 5%. Light shaded regions are greater than 10% and dark shaded regions are greater than 20%.

Figure 16. Same as Fig. 15 for $\overline{Z}_{MF(t)}$. Shading intervals at 10%, 20%, 30%, and 35%.

Figure 17. Difference in percent average explained variance of $\overline{Z}_{MF(t)}$ by the M index from (a) Niño 3 and (b) NP index in the monsoon onset period. Contour interval is 5%. Values greater than 5% are shaded light and values greater than 10% are shaded dark.

Figure 18. Same as Fig. 15 for $\overline{Z}_{MFC(t)}$. Values greater than 5% are shaded light and values greater than 10% are shaded dark.

Figure 19. Average correlation (r) of Niño 3 with $\overline{Z}_{\Phi_{500}(t)}$ in the monsoon onset period with (a) no lag in Niño 3 (time coincident), (b) two month lag, (c) three month lag, and (d) four month lag. Contour interval is 0.1 and absolute values less than 0.2 are not

shown. Dark and light shaded regions indicate statistical significance at the 90% level by the two-tailed student's t-test.

Figure 20. Same as Fig. 19 for NP index with (a) no lag and (b) two month lag.

Figure 21. Same as Fig. 19 for M index with (a) no lag and (b) two month lag.

Figure 22. Idealized relationship of monsoon ridge position and mid-level moisture transport to Pacific SSTs at monsoon onset.

XII. LIST OF TABLES

Table 1. Frequently used acronyms and symbols.

Acronym or symbol	Meaning
CNP	Central North Pacific region (177° E-164° W, 26-36° N)
ENSO	El Niño Southern Oscillation
ENP	Eastern North Pacific region (125-150° W, 35-50° N)
LLJ	Low level jet
M	North American Monsoon sea surface temperature index
MF	Integrated moisture flux (sigma levels 14-28)
MFC	Integrated moisture flux convergence (sigma levels 14-28)
NAM	North American Monsoon
NP	North Pacific sea surface temperature index
NPO	North Pacific Oscillation
PR	Regional Precipitation index
PT	Pacific Transition Pattern
r	Correlation coefficient
r^2	Explained variance
SPI	Standardized precipitation index
SST	Sea surface temperature
SSTA	Normalized sea surface temperature anomaly
$\overline{Z}_{\chi(t)}$	Thirty-day average Z-score of reanalysis variable χ centered on the date
Φ_{500}	500-mb geopotential height

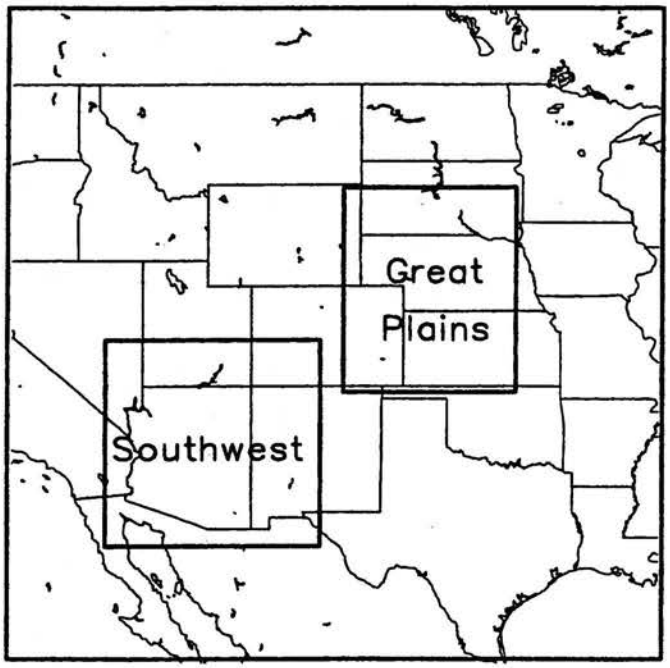

Figure 1.

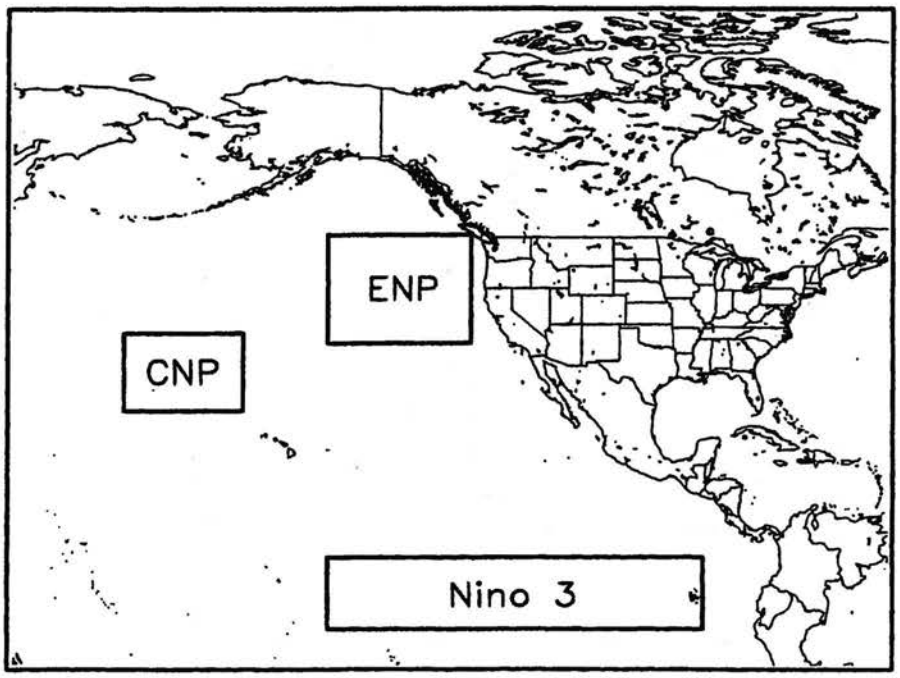

Figure 2.

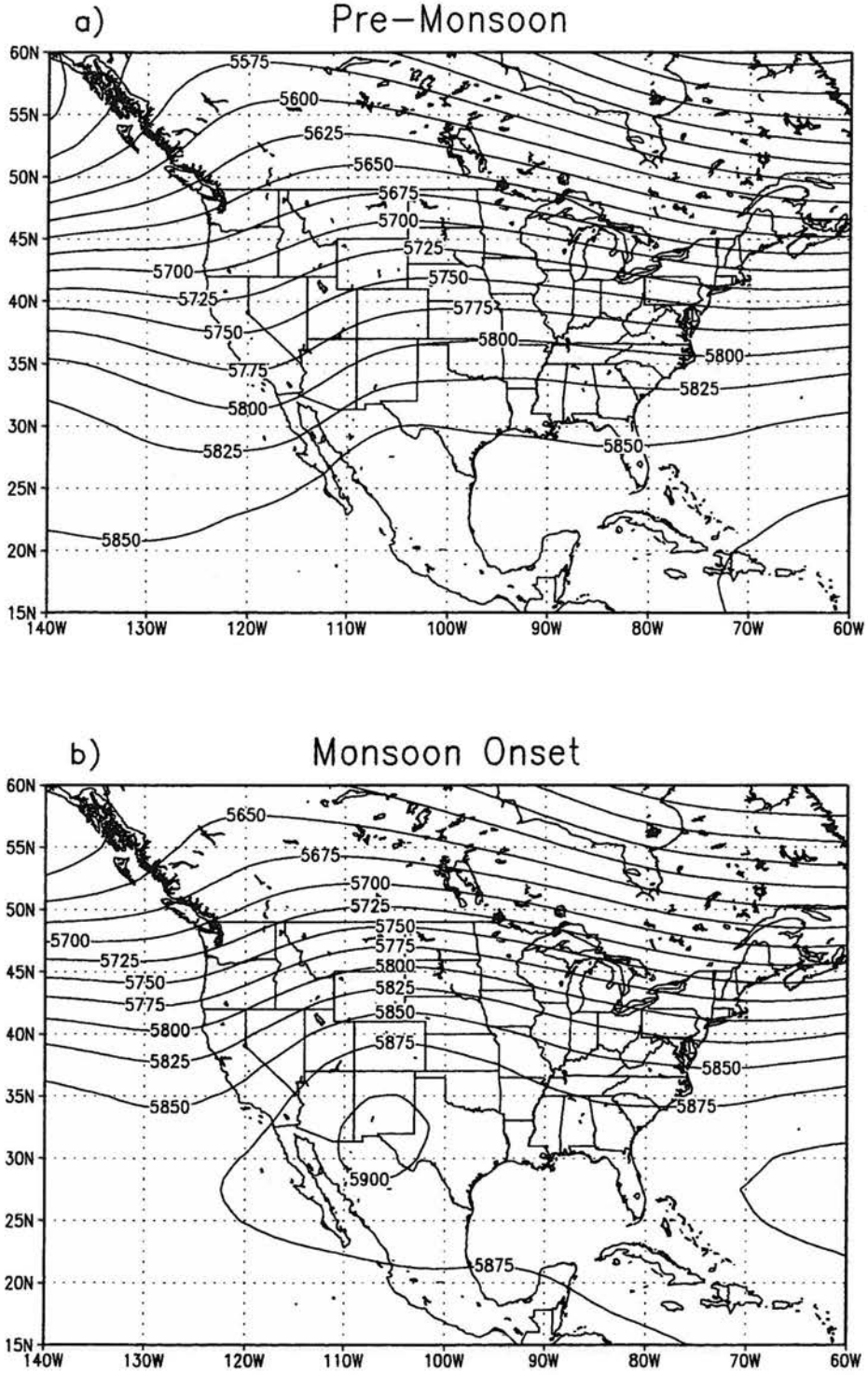

Figure 3. a) and b)

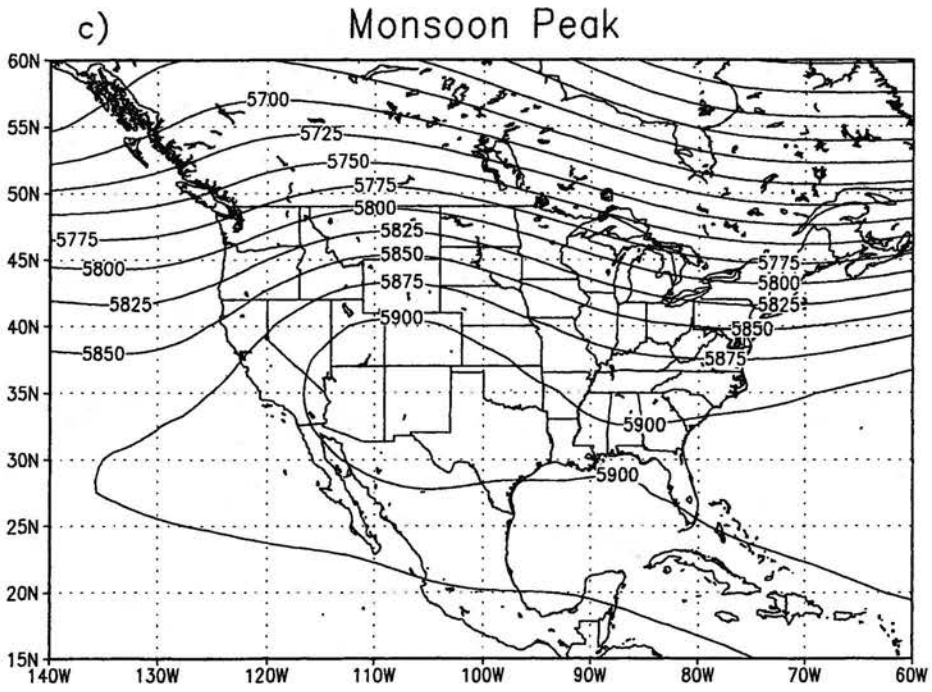

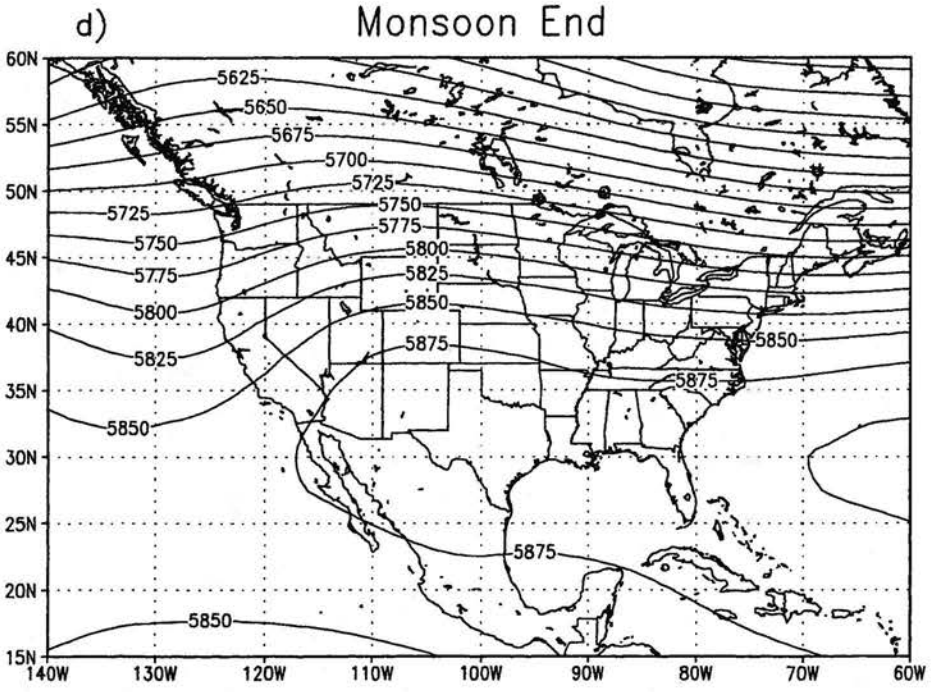

Figure 3. c) and d)

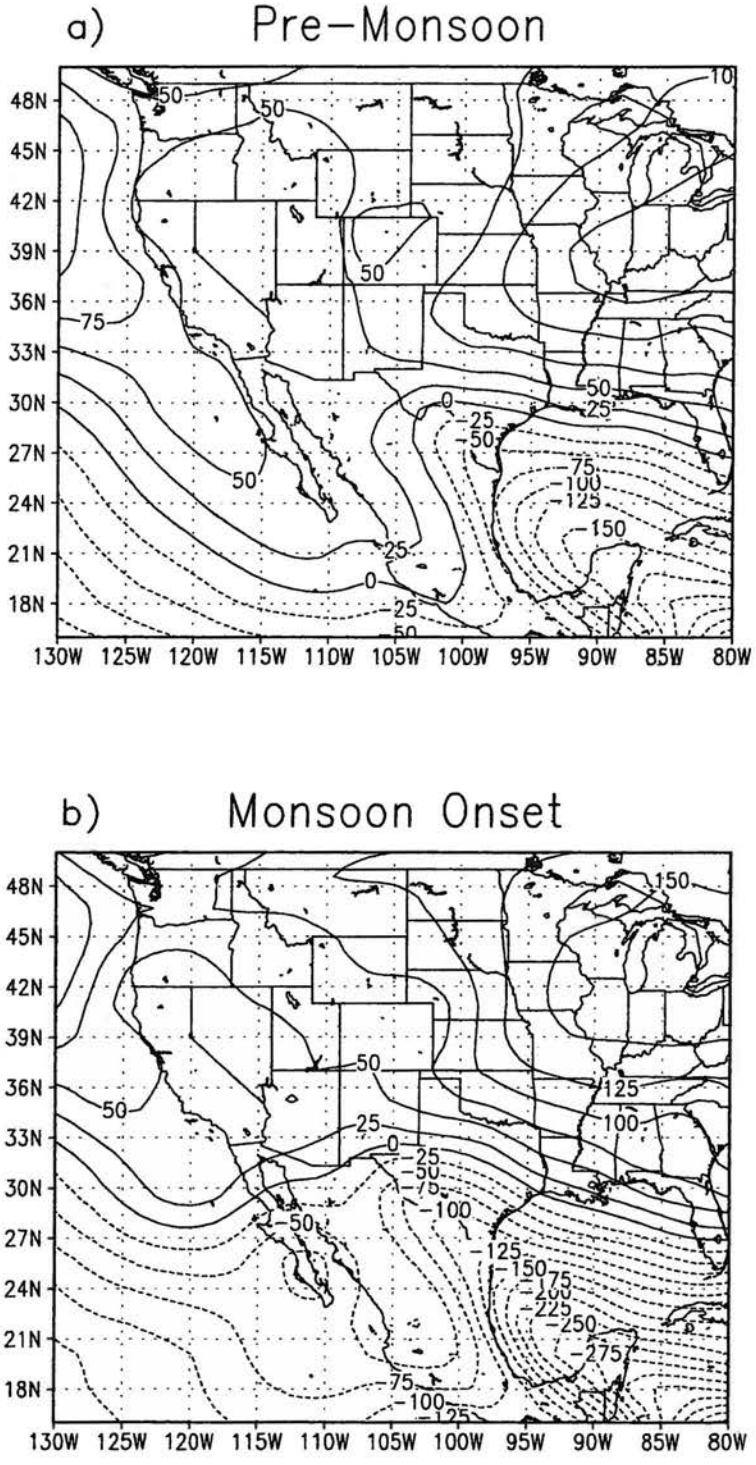

Figure 4. a) and b)

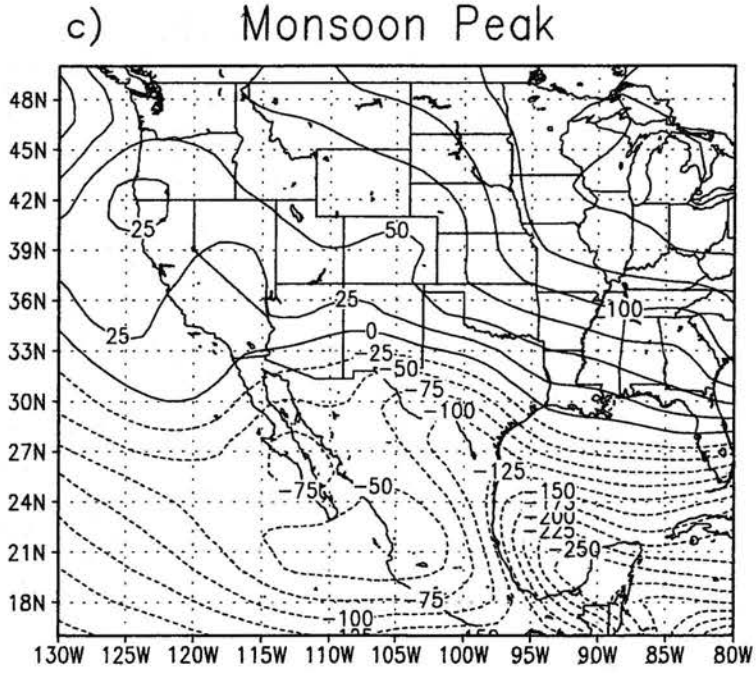

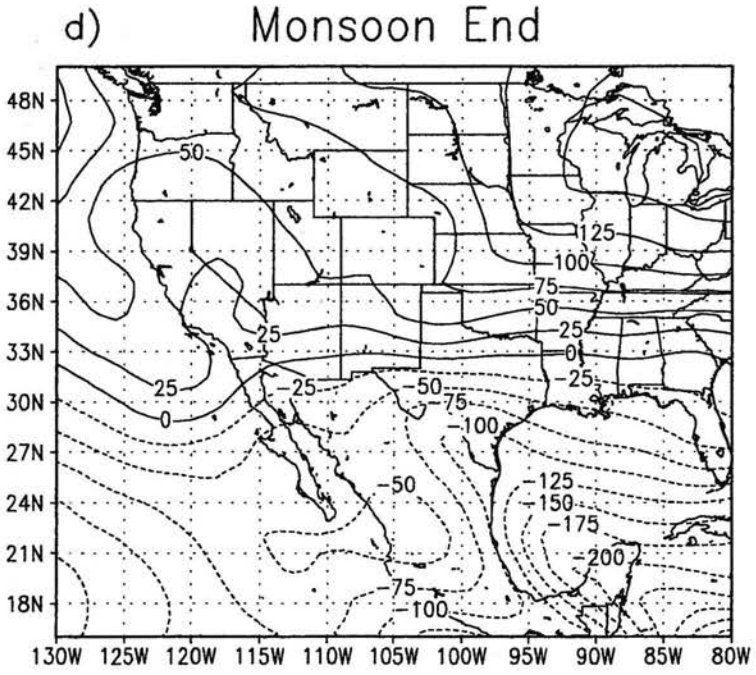

Figure 4. c) and d)

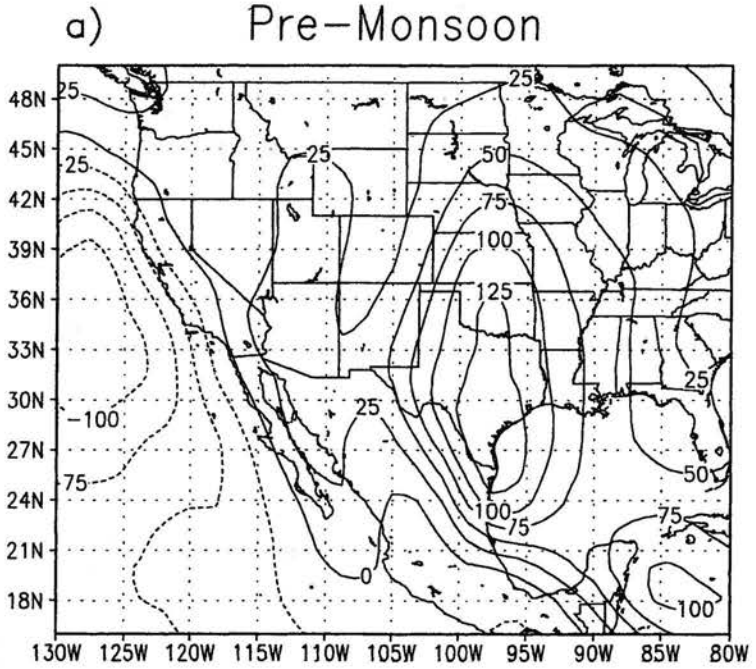

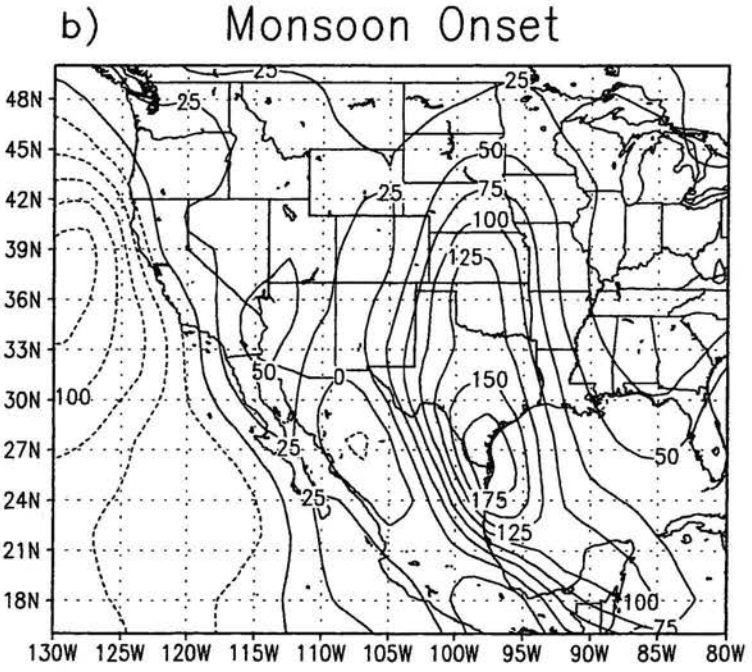

Figure 5. a) and b)

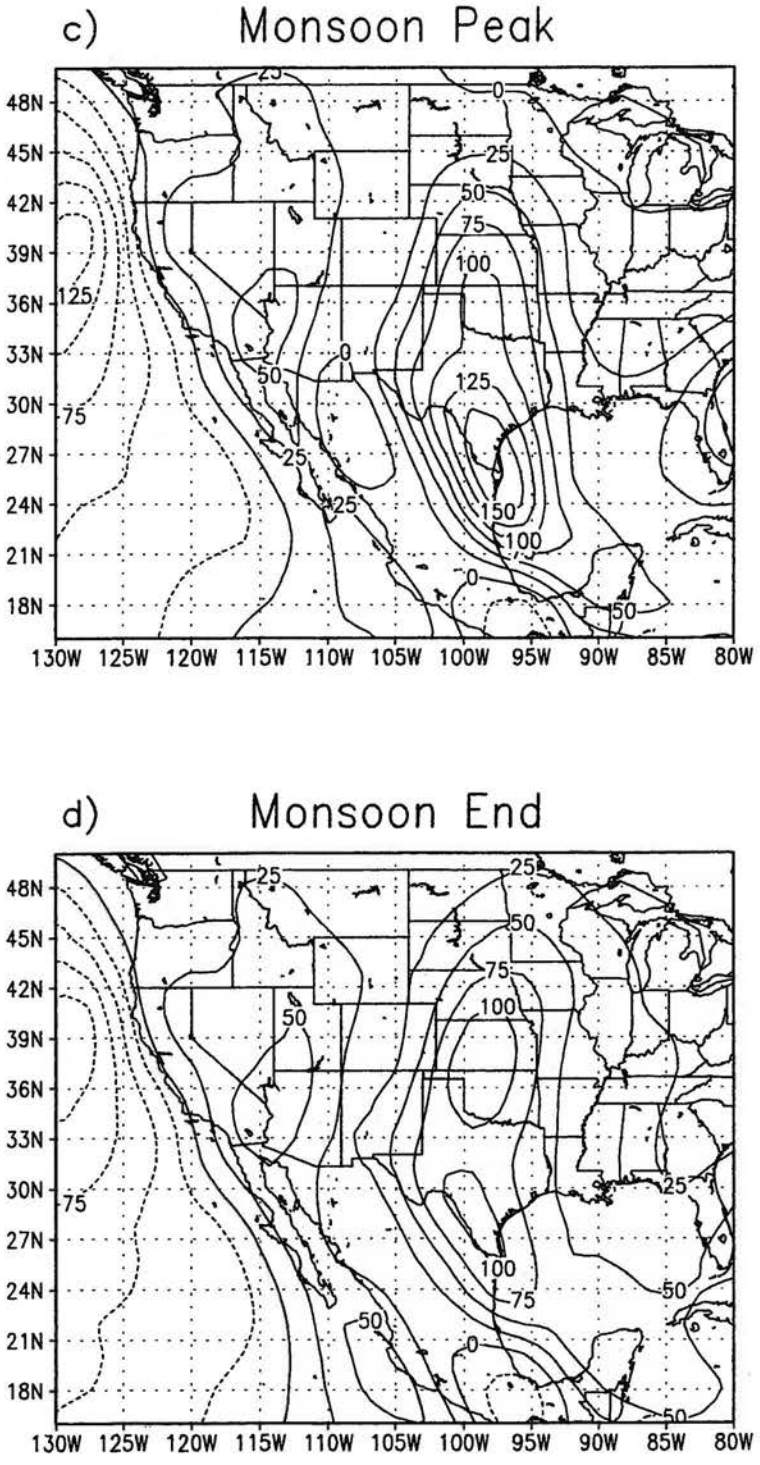

Figure 5. c) and d)

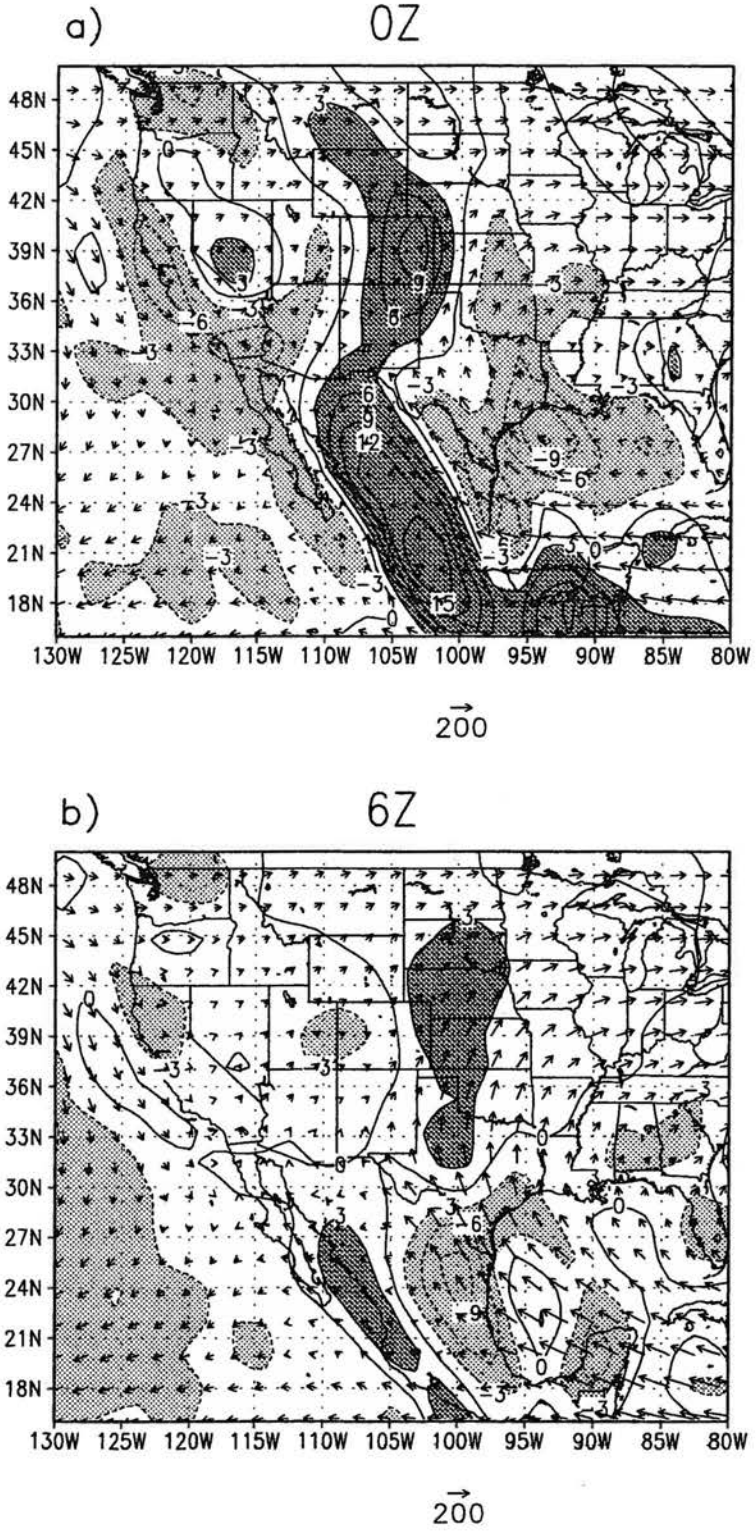

Figure 6. a) and b)

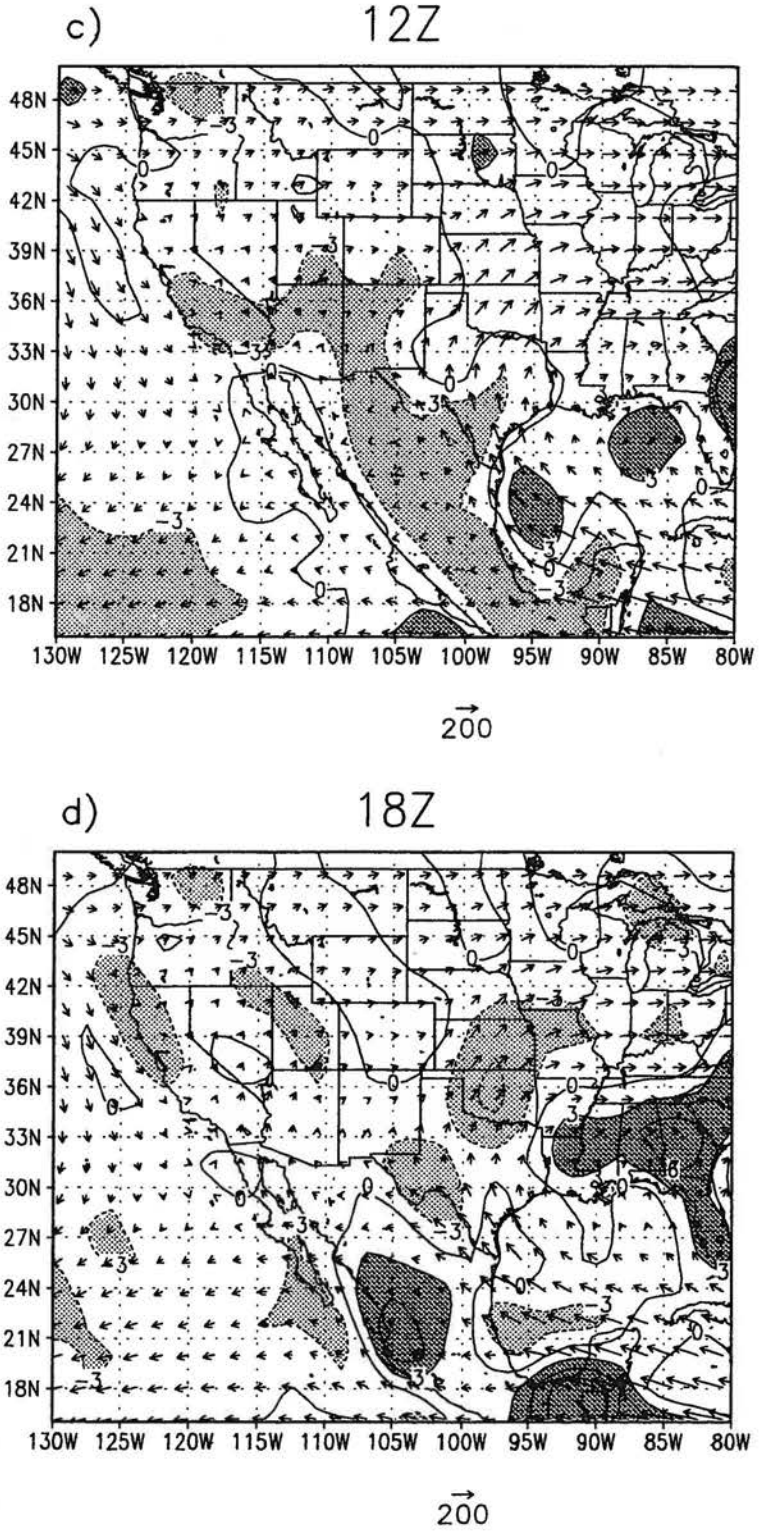

Figure 6. c) and d)

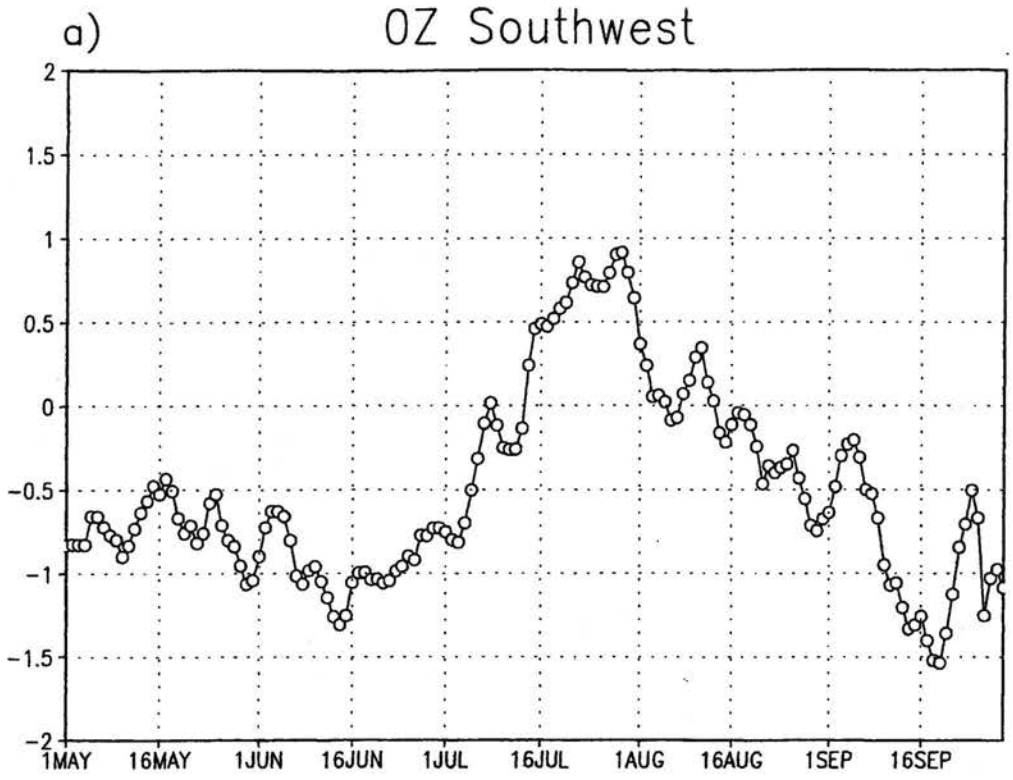

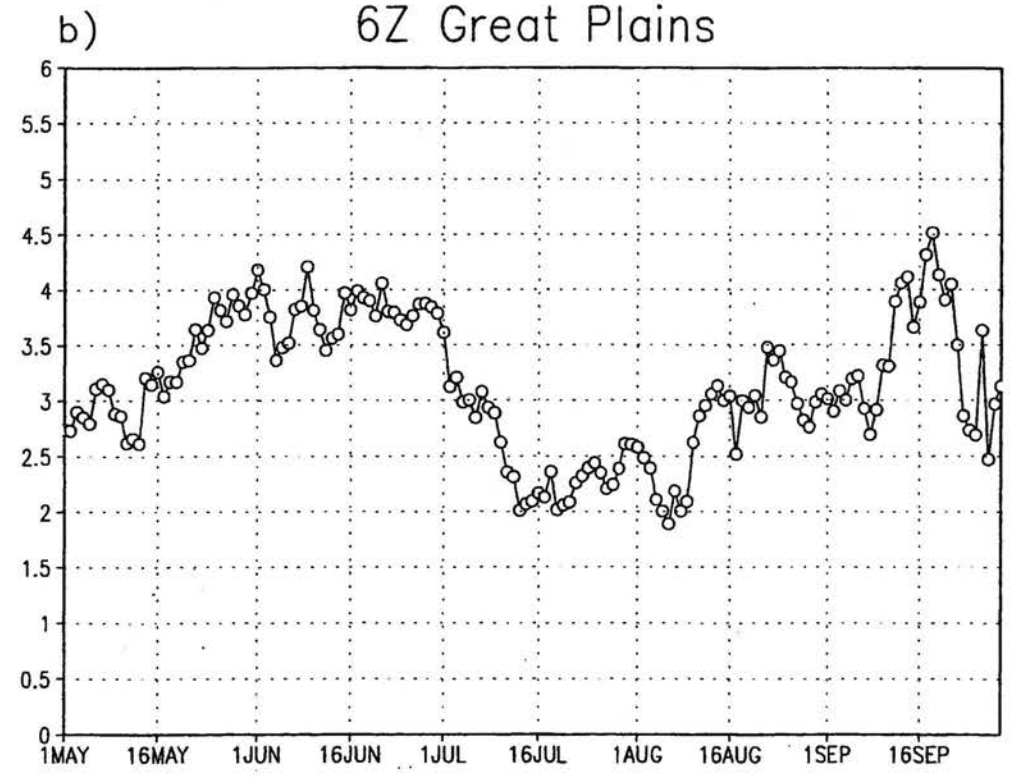

Figure 7. a) and b)

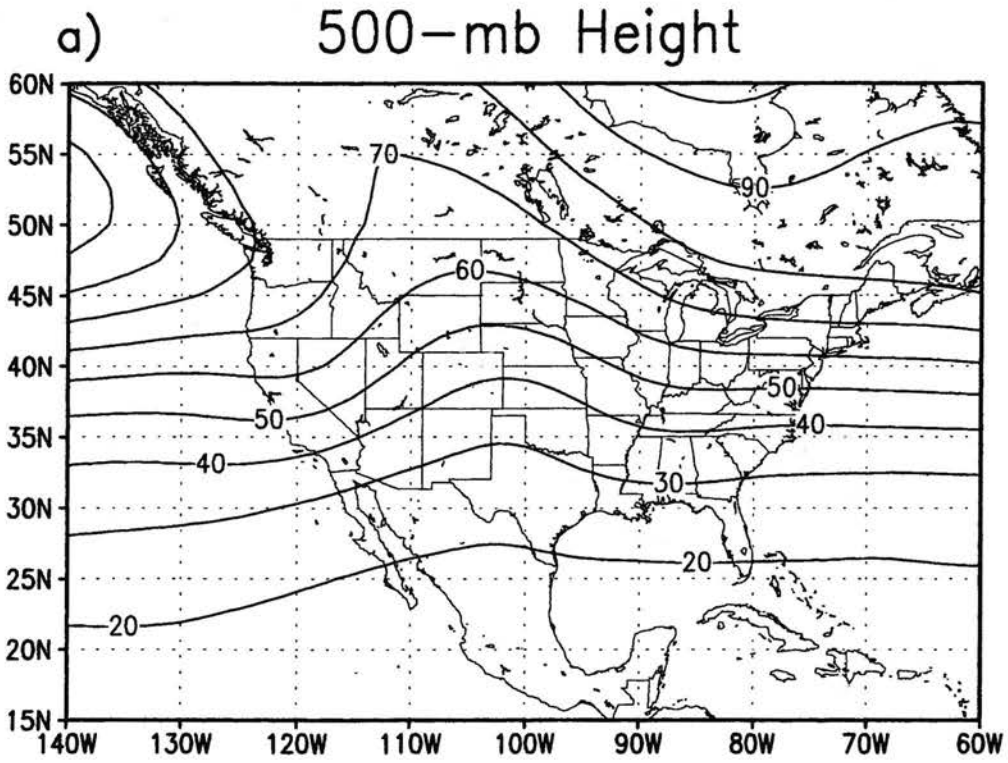
a)
500−mb Height
60N
55N
50N
45N
40N
35N
30N
25N
20N
15N
140W
130W
120W
110W
100W
90W
80W
70W
60W
70
90
60
50
40
50
40
30
20
20

Figure 8. a)

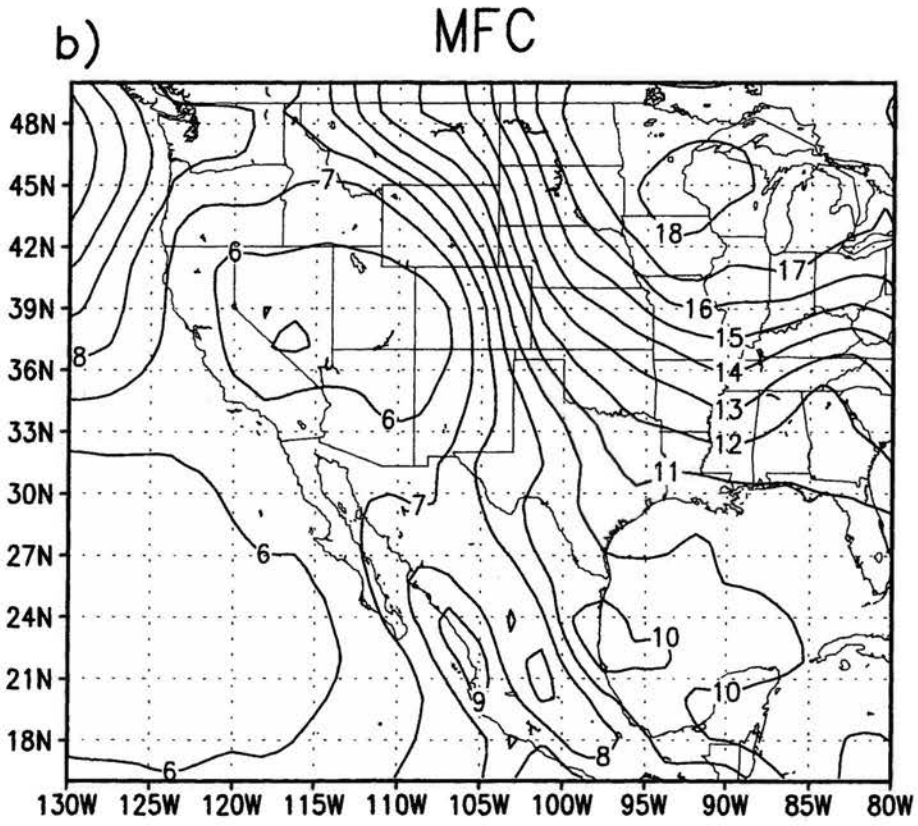
b)
MFC
48N
45N
42N
39N
36N
33N
30N
27N
24N
21N
18N
130W
125W
120W
115W
110W
105W
100W
95W
90W
85W
80W
6
7
8
9
10
11
12
13
14
15
16
17
18

Figure 8. b)

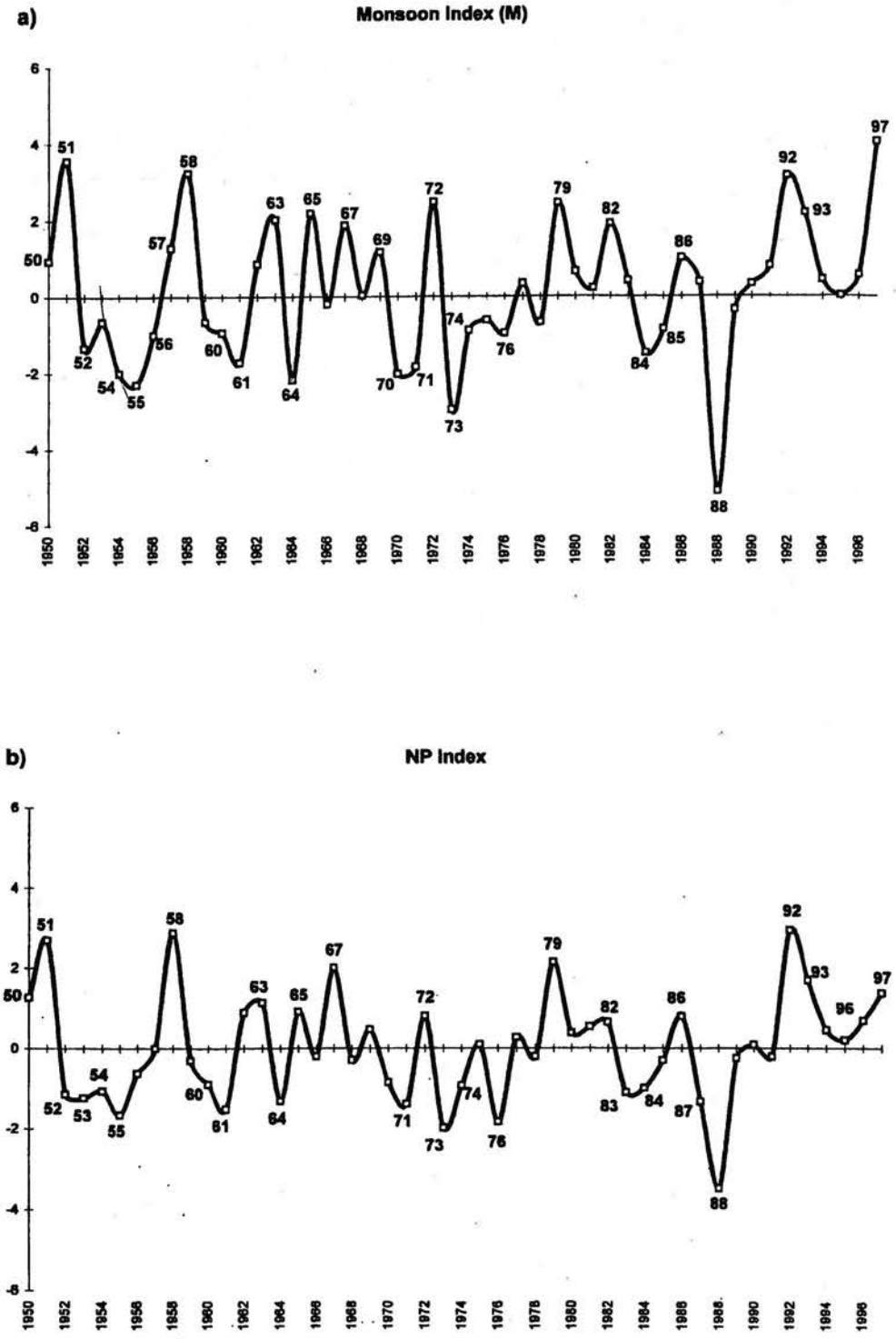

Figure 9. a) and b)

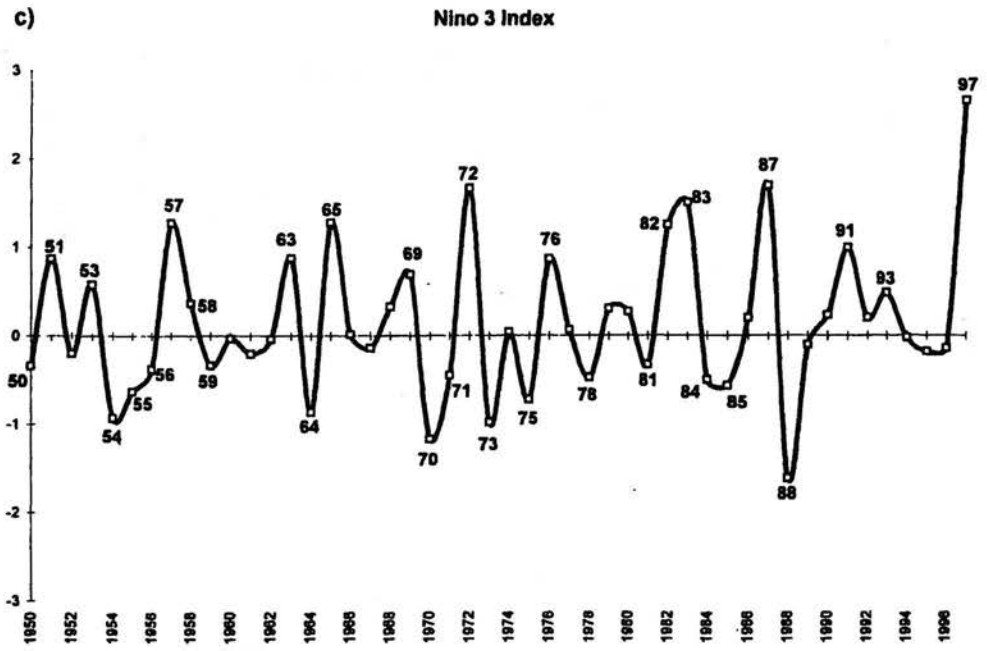
c)
Nino 3 Index
3
2
1
0
-1
-2
-3
50
51
53
54
55
56
57
58
59
63
64
65
69
70
71
72
73
75
76
78
81
82
83
84
85
87
88
91
93
97
1950
1952
1954
1956
1958
1960
1962
1964
1966
1968
1970
1972
1974
1976
1978
1980
1982
1984
1986
1988
1990
1992
1994
1996

Figure 9. c)

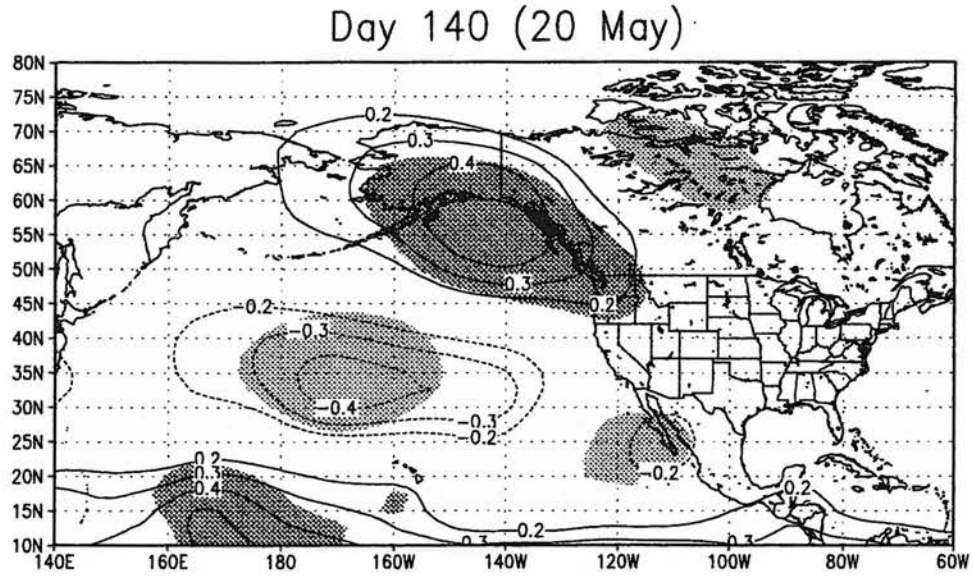
Day 140 (20 May)
80N
75N
70N
65N
60N
55N
50N
45N
40N
35N
30N
25N
20N
15N
10N
140E
160E
180
160W
140W
120W
100W
80W
60W

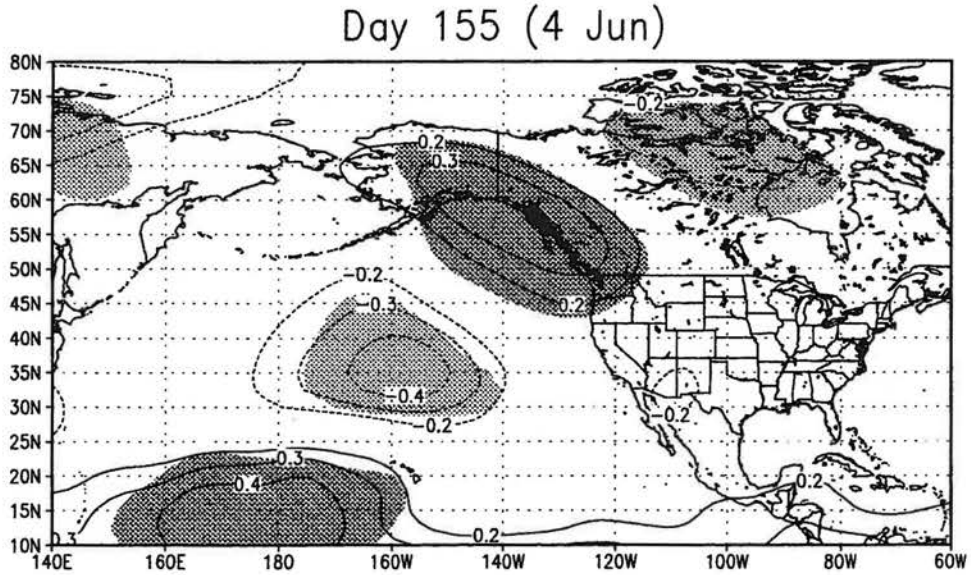
Day 155 (4 Jun)
80N
75N
70N
65N
60N
55N
50N
45N
40N
35N
30N
25N
20N
15N
10N
140E
160E
180
160W
140W
120W
100W
80W
60W

Figure 10.

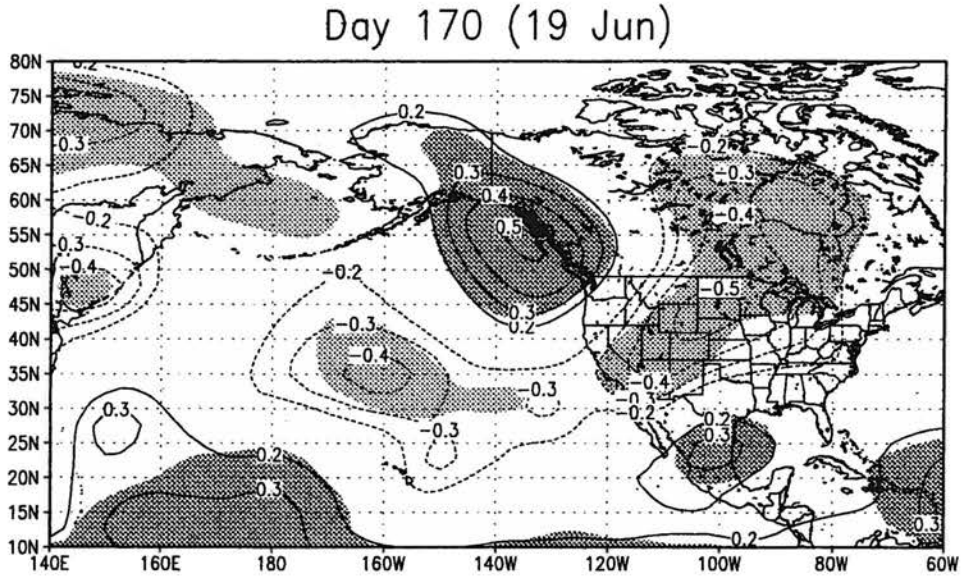

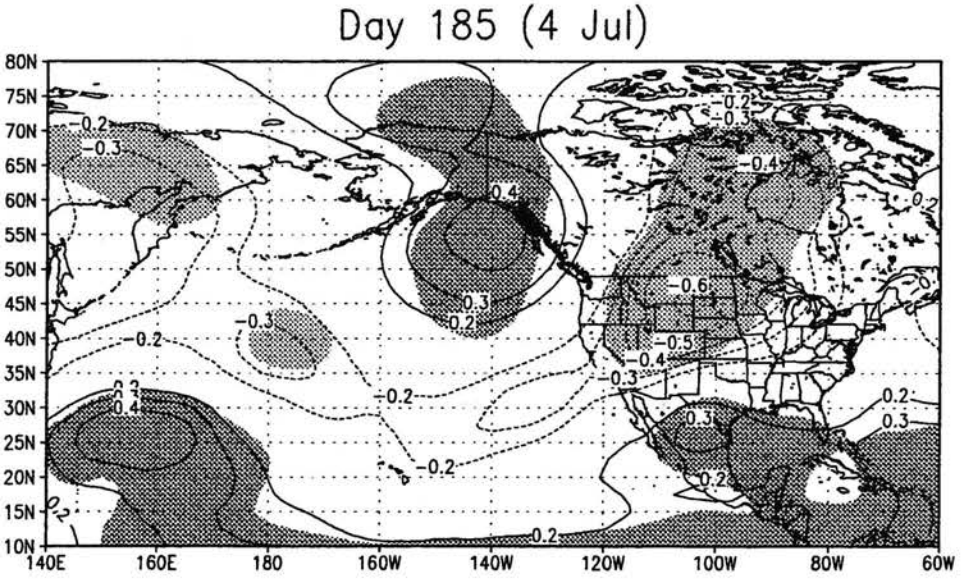

Figure 10. continued

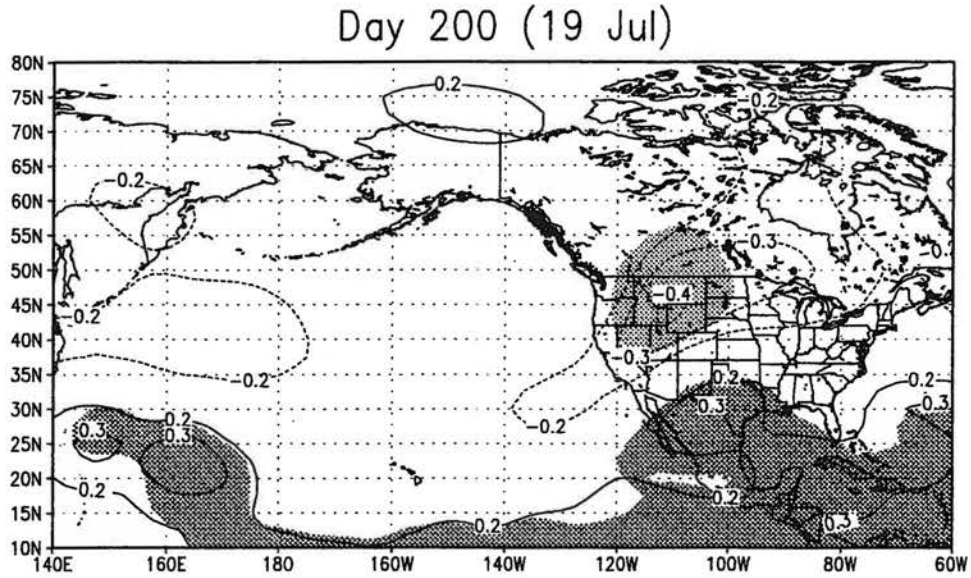

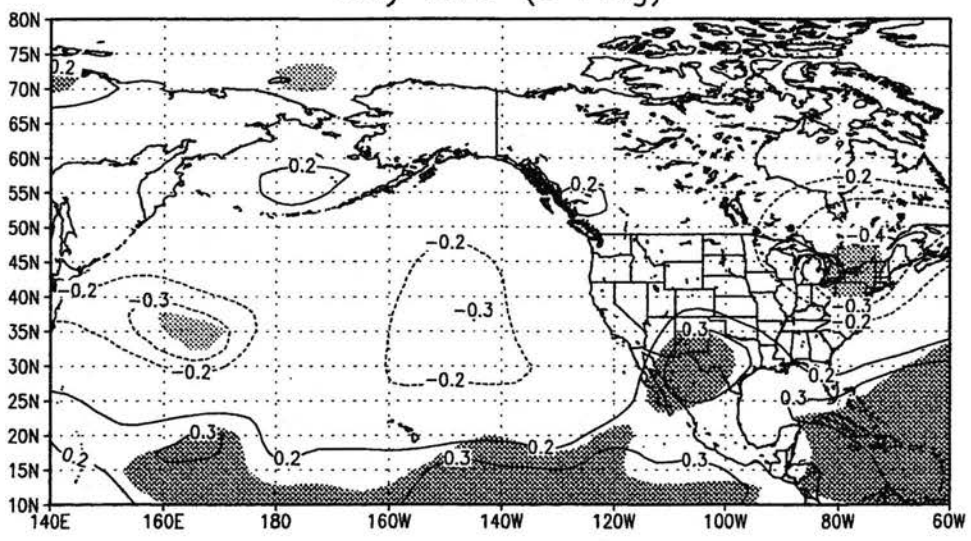

Figure 10. continued

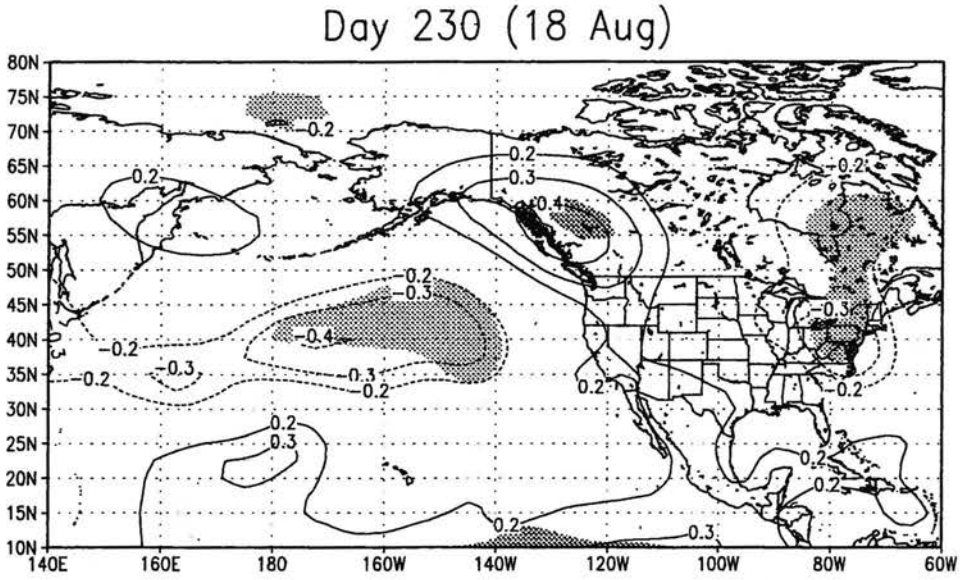

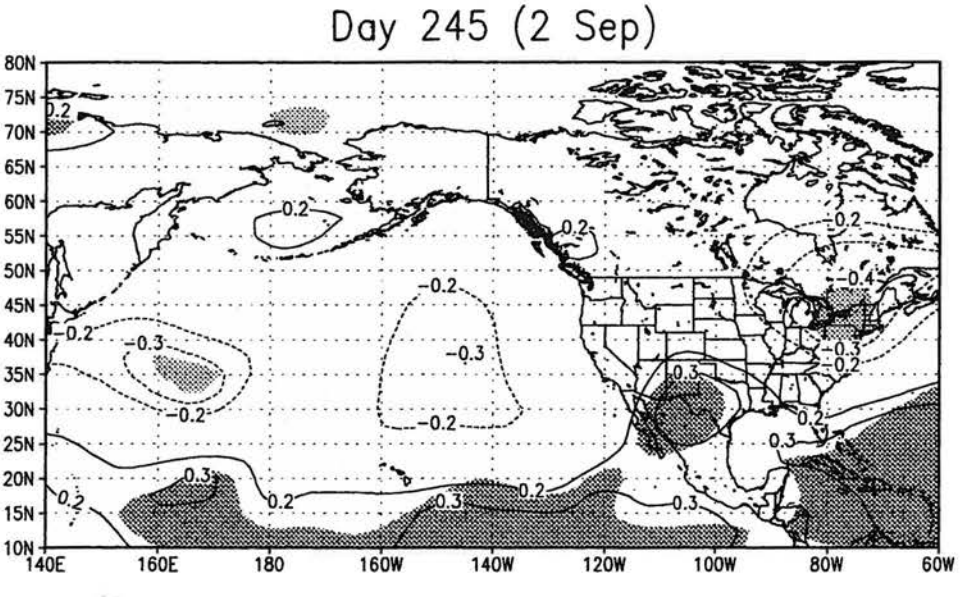

Figure 10. continued

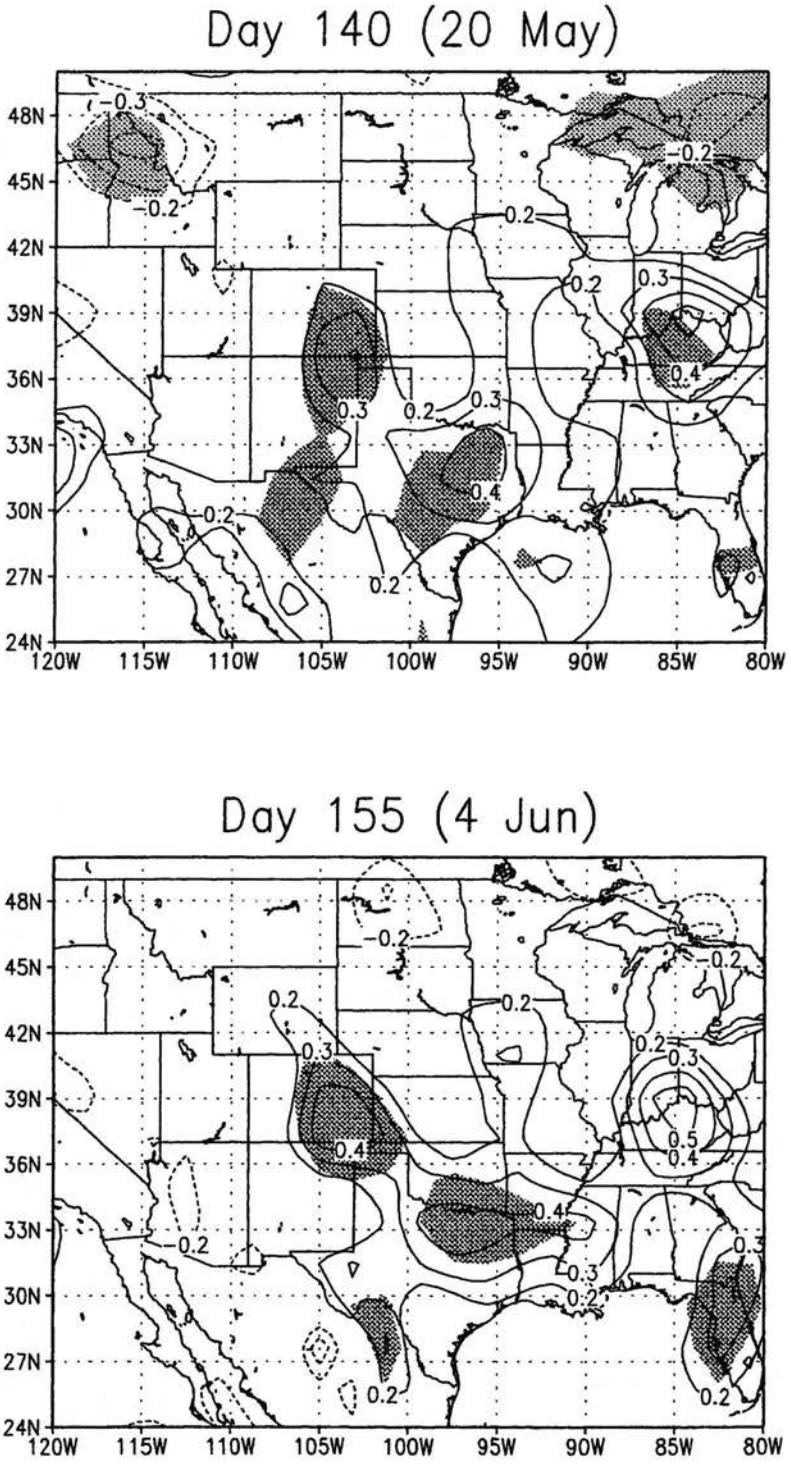
Day 140 (20 May)
Day 155 (4 Jun)
48N
45N
42N
39N
36N
33N
30N
27N
24N
120W
115W
110W
105W
100W
95W
90W
85W
80W

Figure 11.

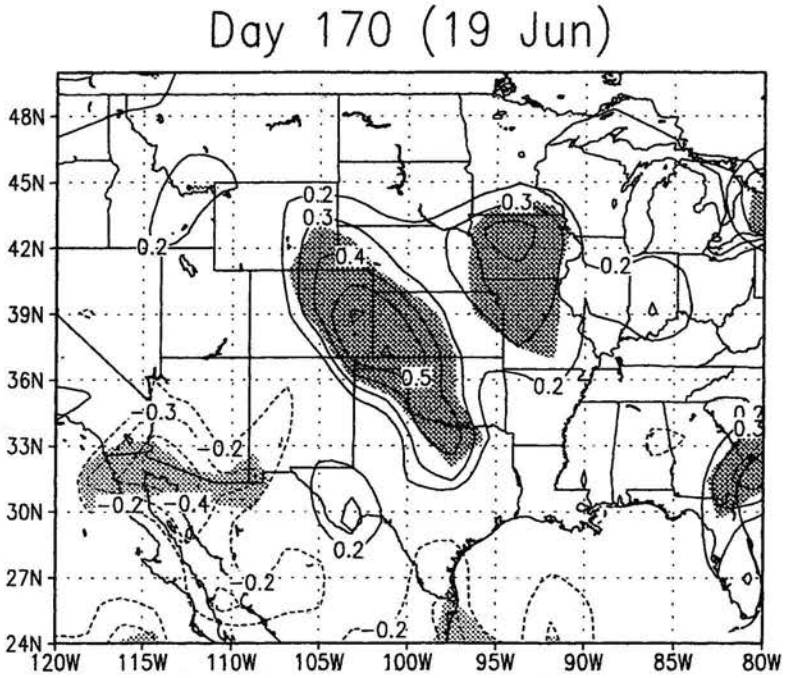

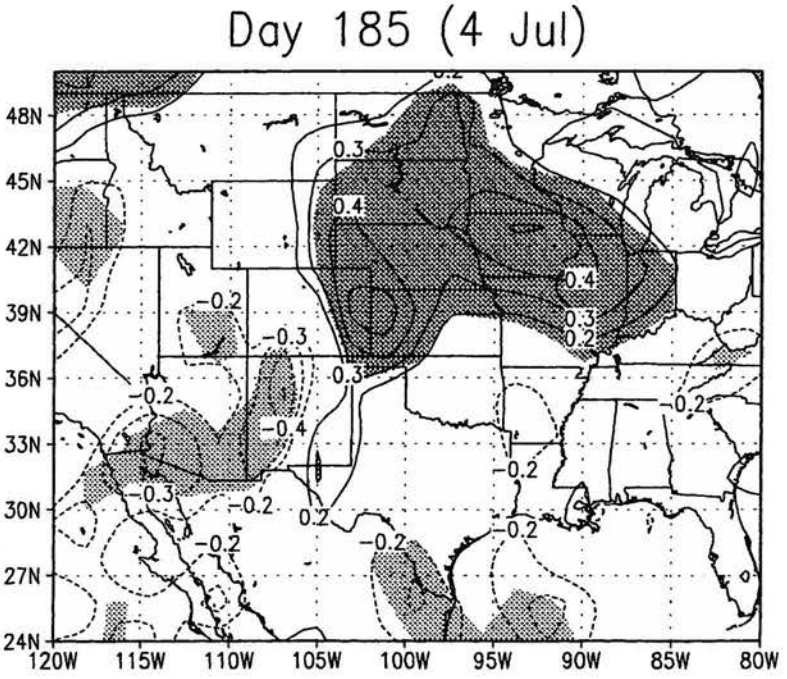

Figure 11. continued

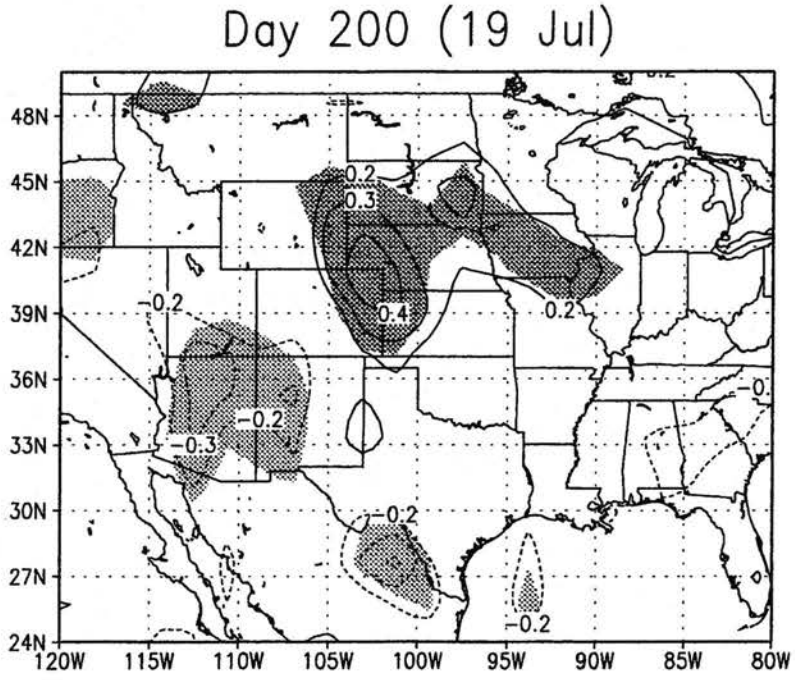

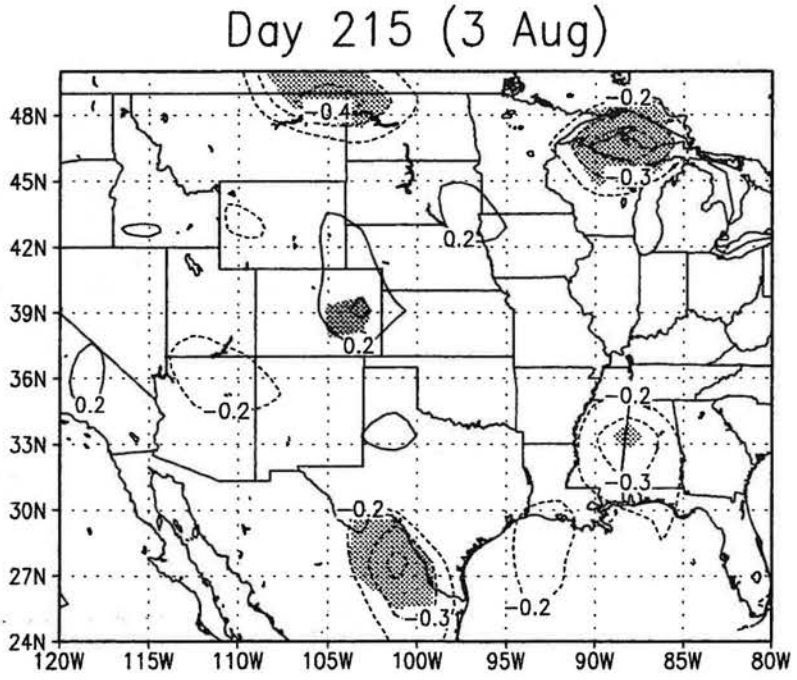

Figure 11. continued

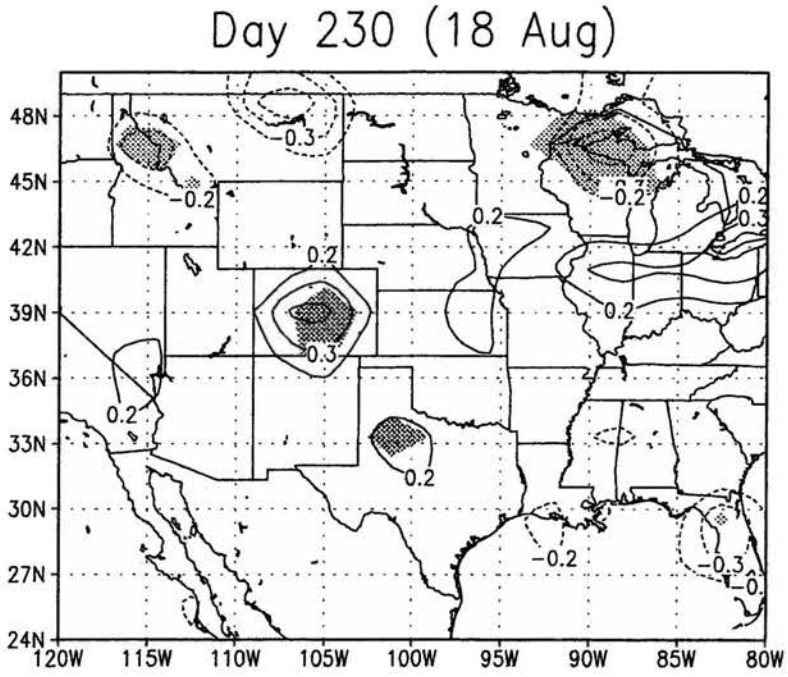

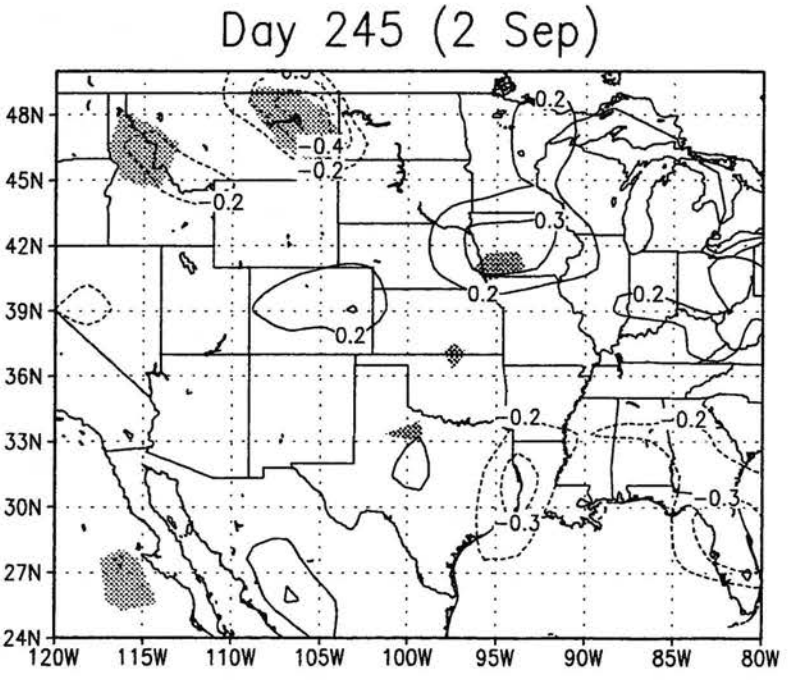

Figure 11. continued

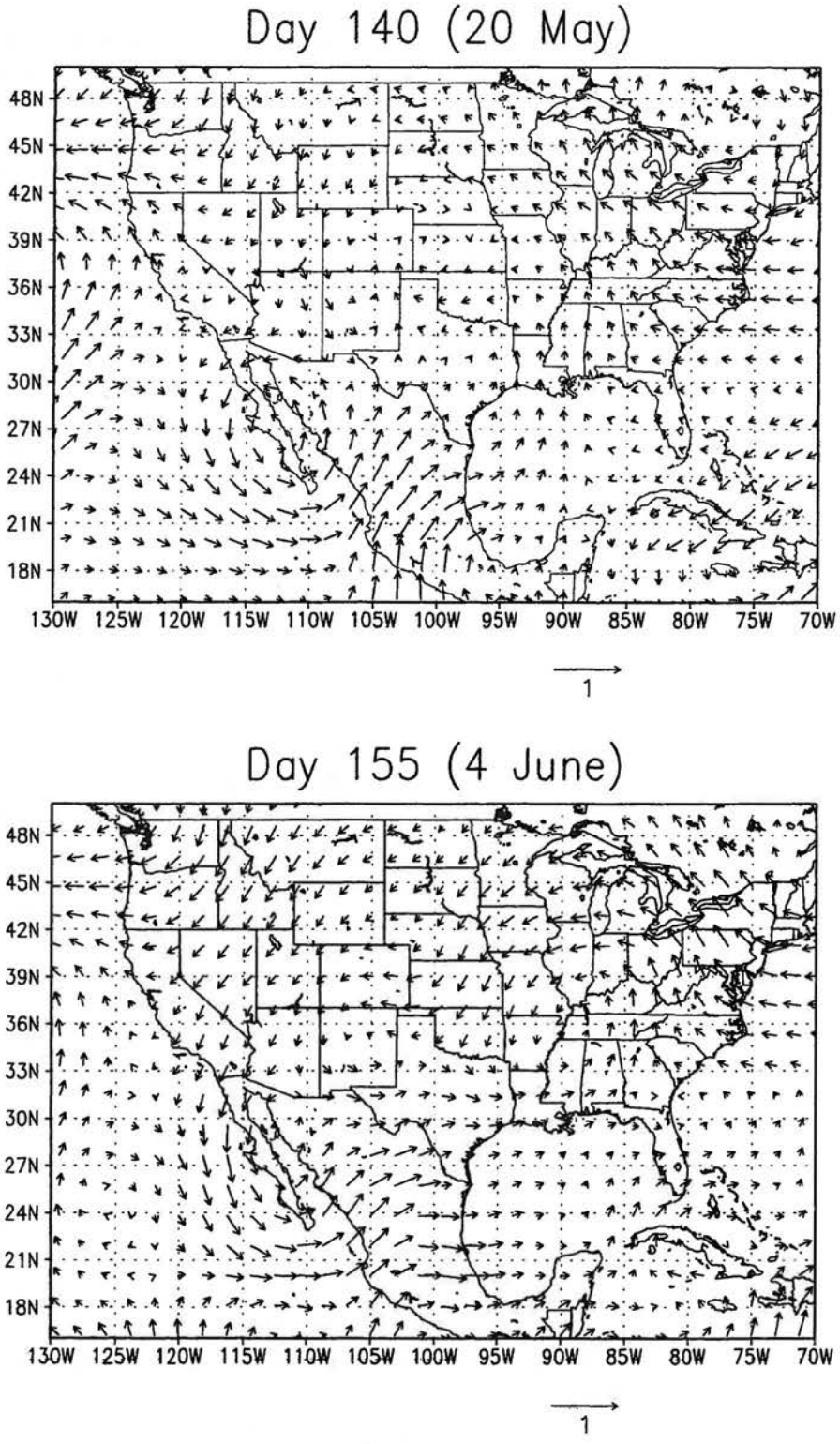
Day 140 (20 May)
48N
45N
42N
39N
36N
33N
30N
27N
24N
21N
18N
130W 125W 120W 115W 110W 105W 100W 95W 90W 85W 80W 75W 70W
1
Day 155 (4 June)
48N
45N
42N
39N
36N
33N
30N
27N
24N
21N
18N
130W 125W 120W 115W 110W 105W 100W 95W 90W 85W 80W 75W 70W
1

Figure 12.

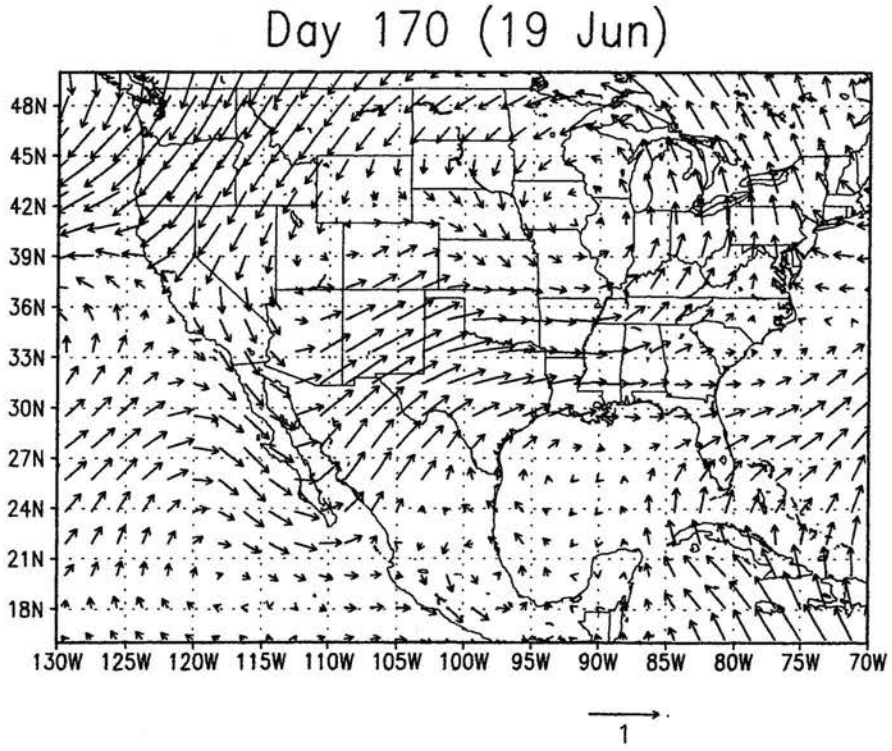

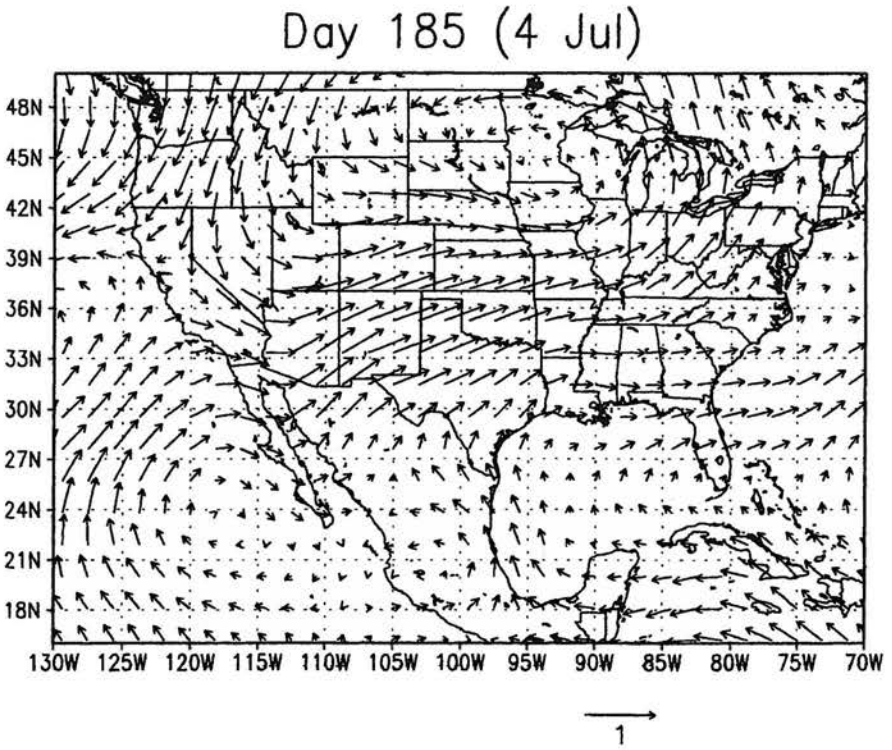

Figure 12. continued

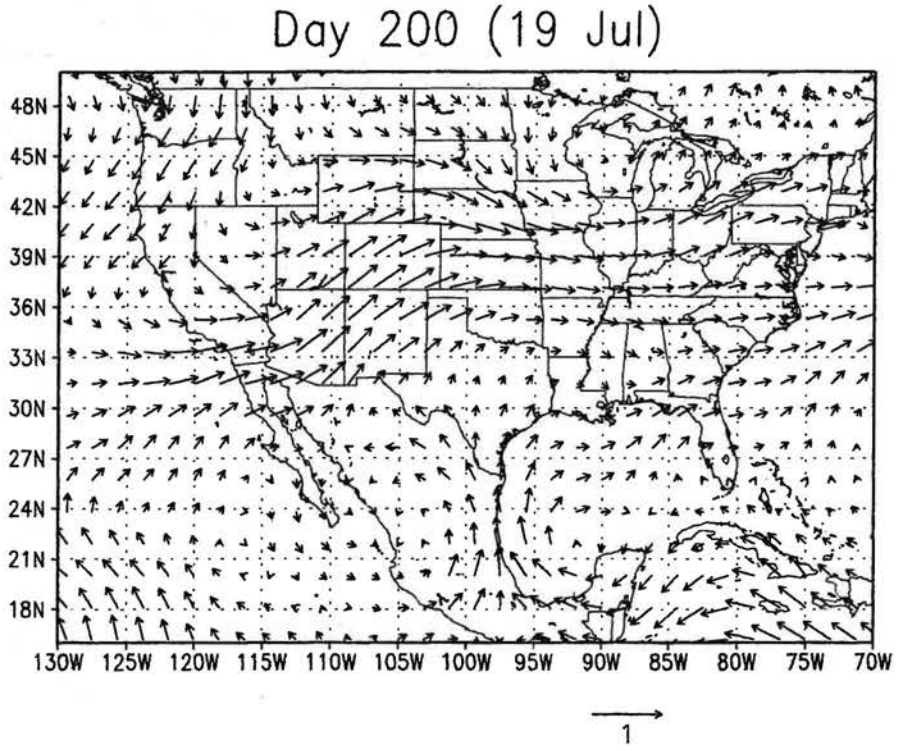

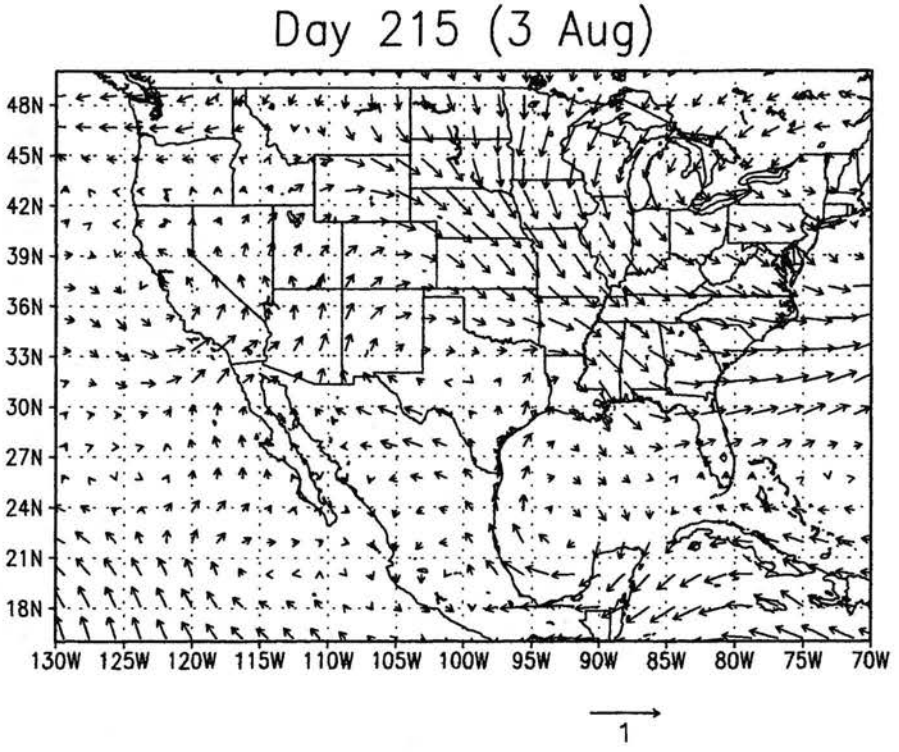

Figure 12. continued

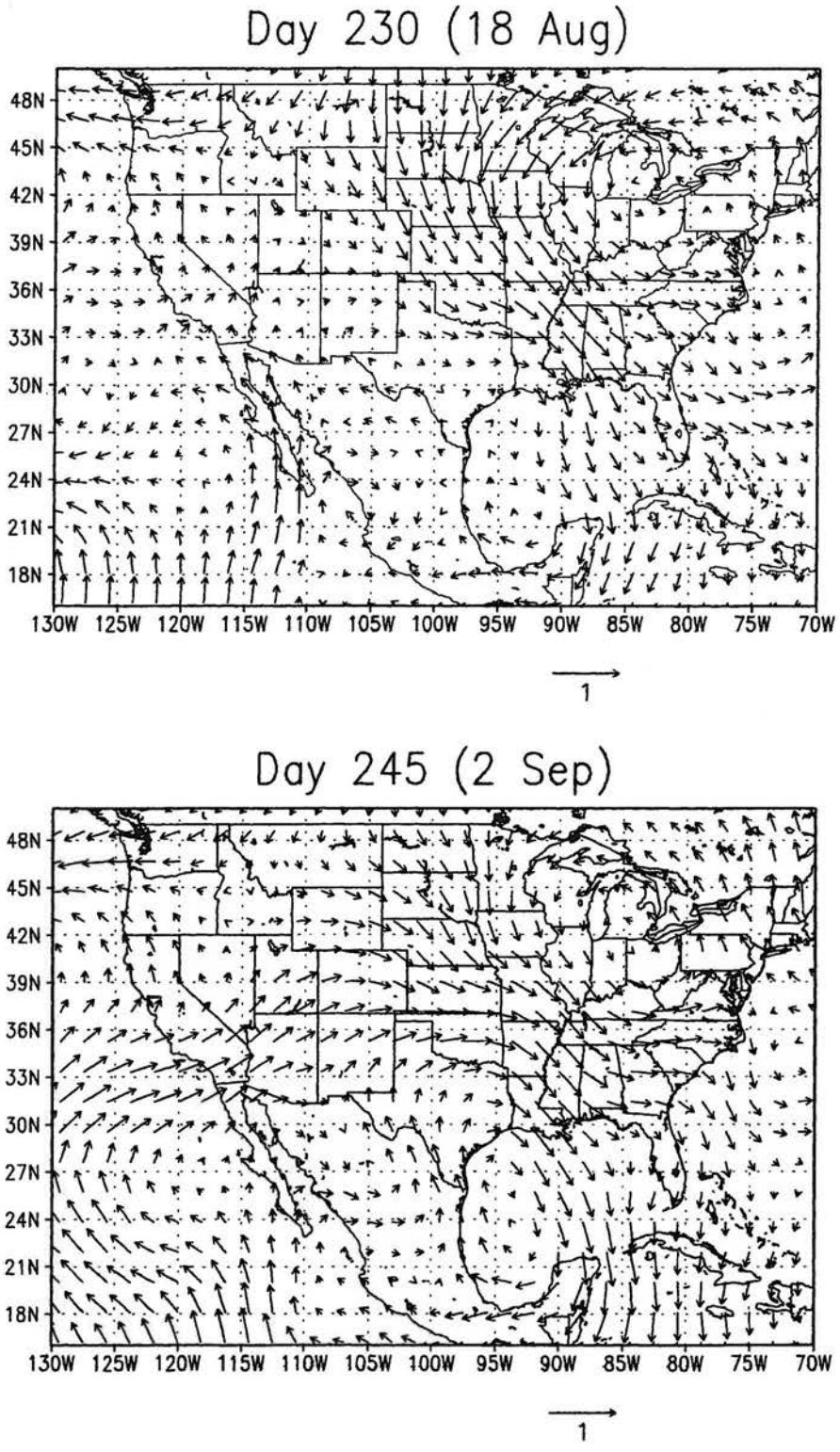

Figure 12. continued

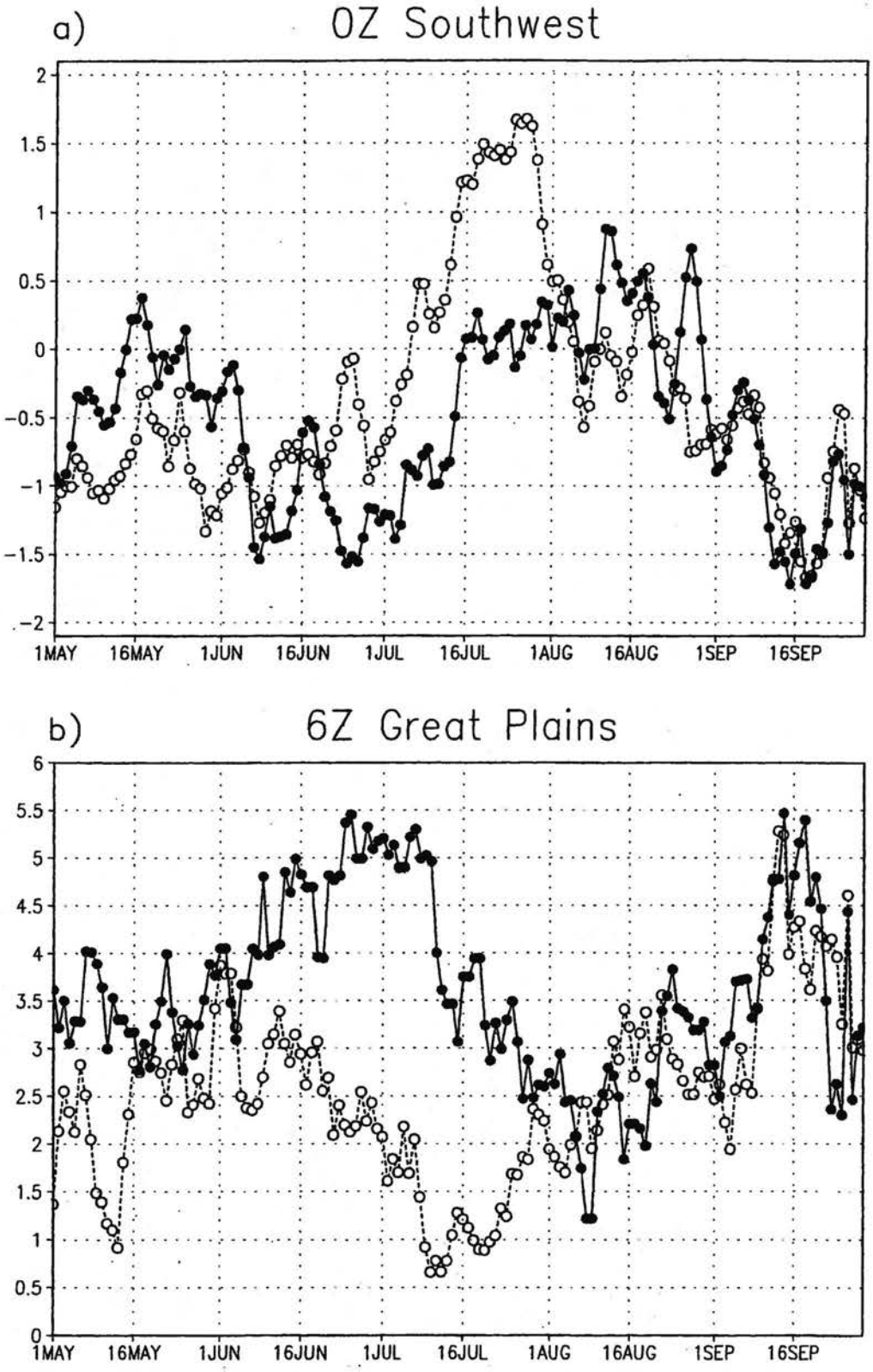

Figure 13. a) and b)

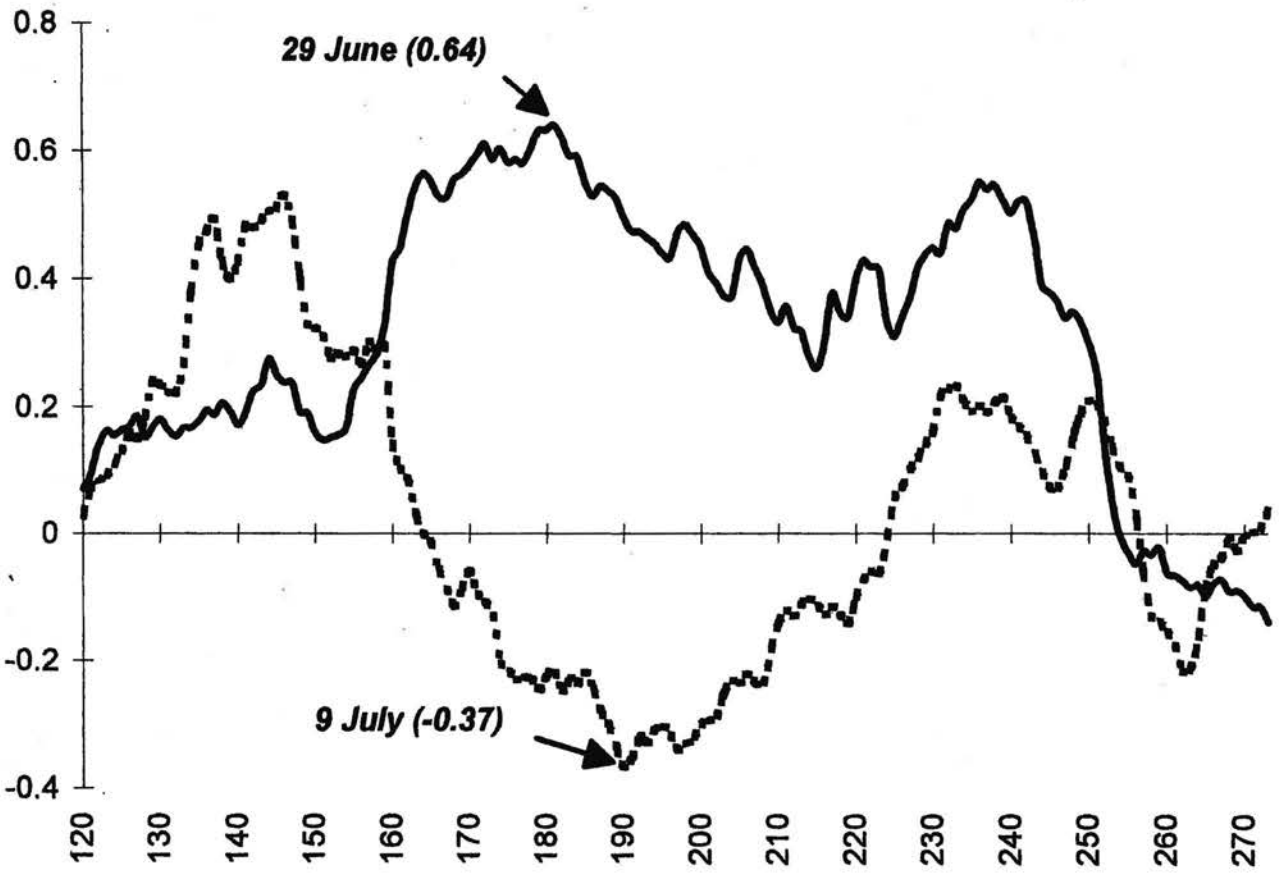
29 June (0.64)
9 July (-0.37)
0.8
0.6
0.4
0.2
0
-0.2
-0.4
120
130
140
150
160
170
180
190
200
210
220
230
240
250
260
270

Figure 14.

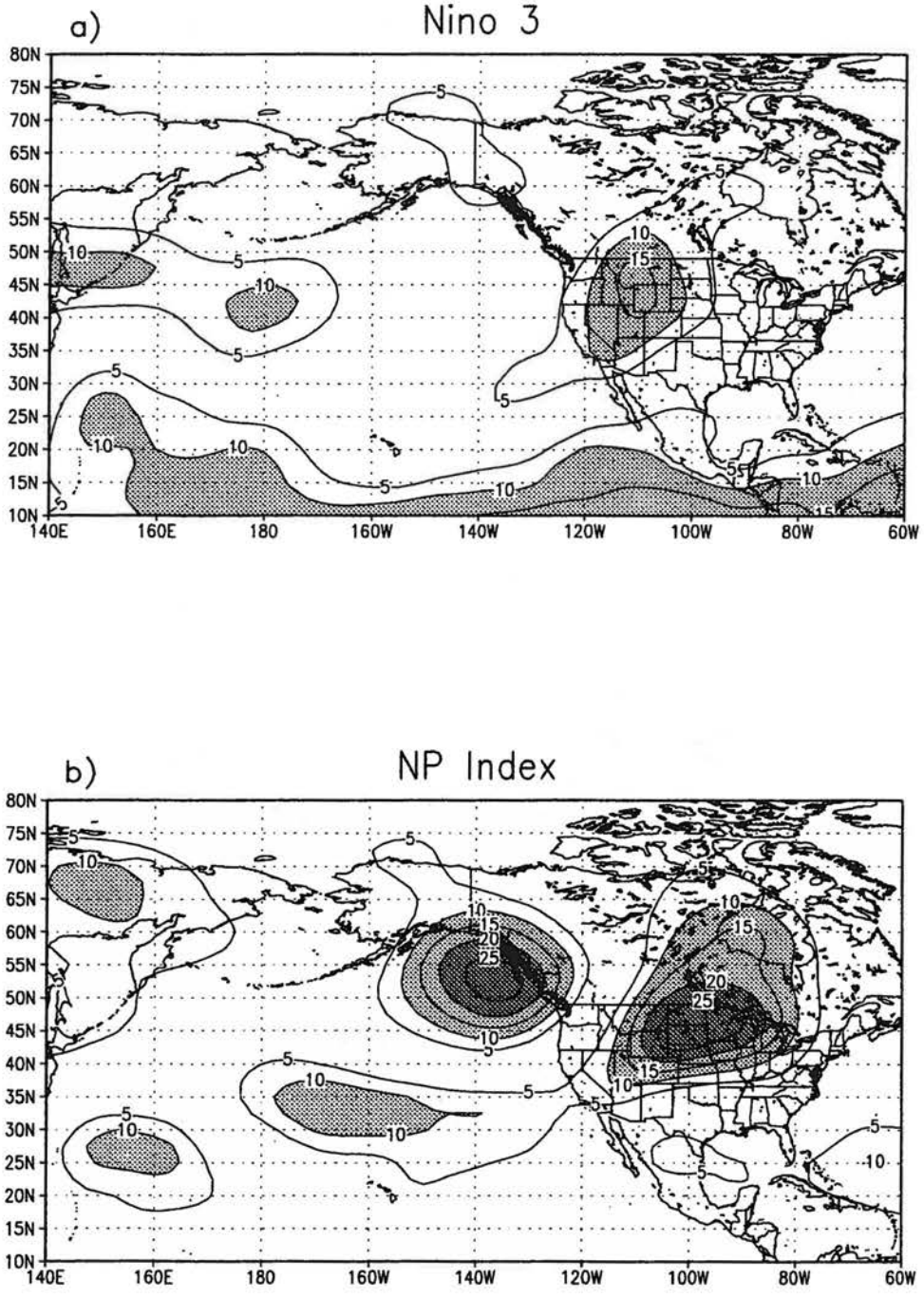

Figure 15. a) and b)

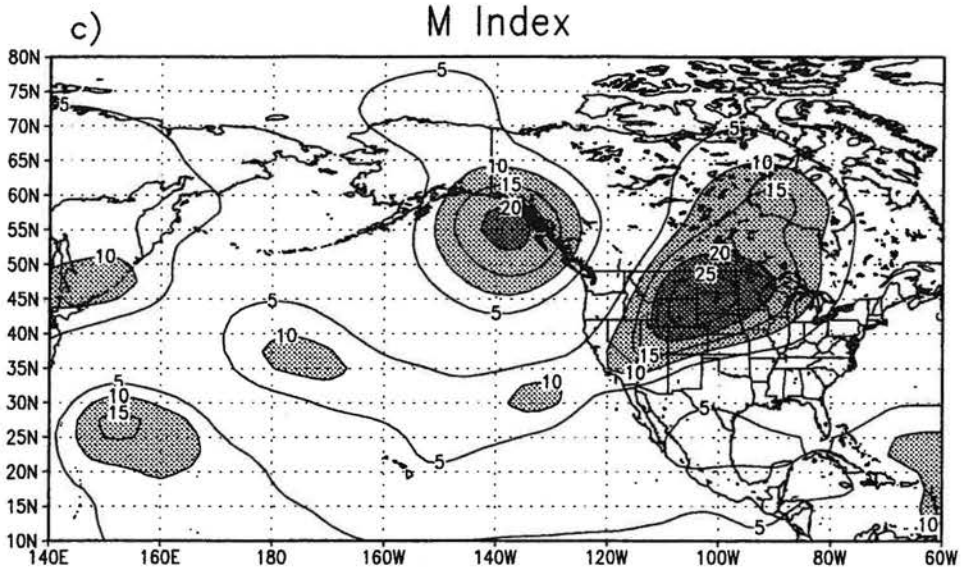
c)
M Index
80N
75N
70N
65N
60N
55N
50N
45N
40N
35N
30N
25N
20N
15N
10N
140E
160E
180
160W
140W
120W
100W
80W
60W

Figure 15. c)

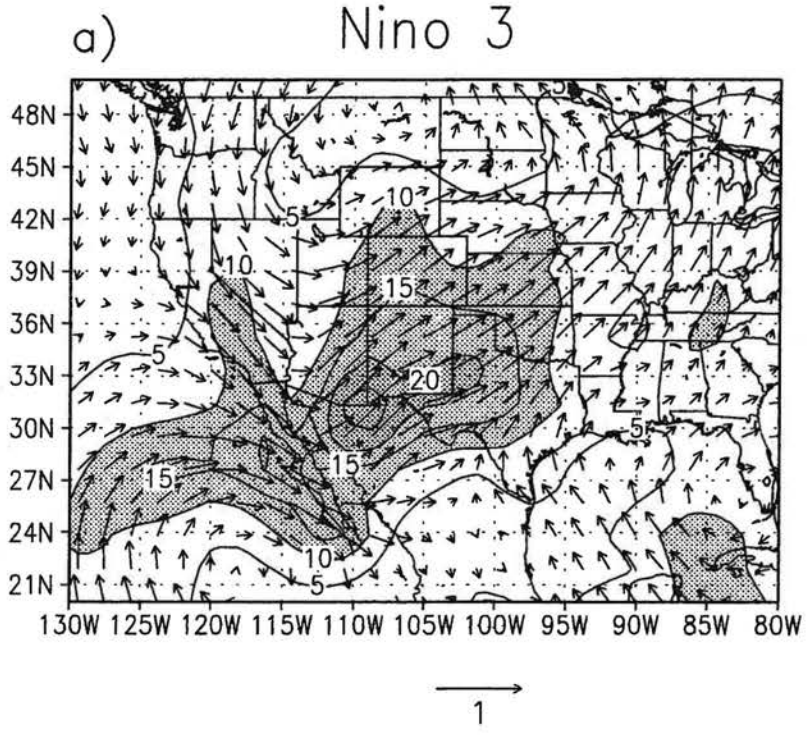

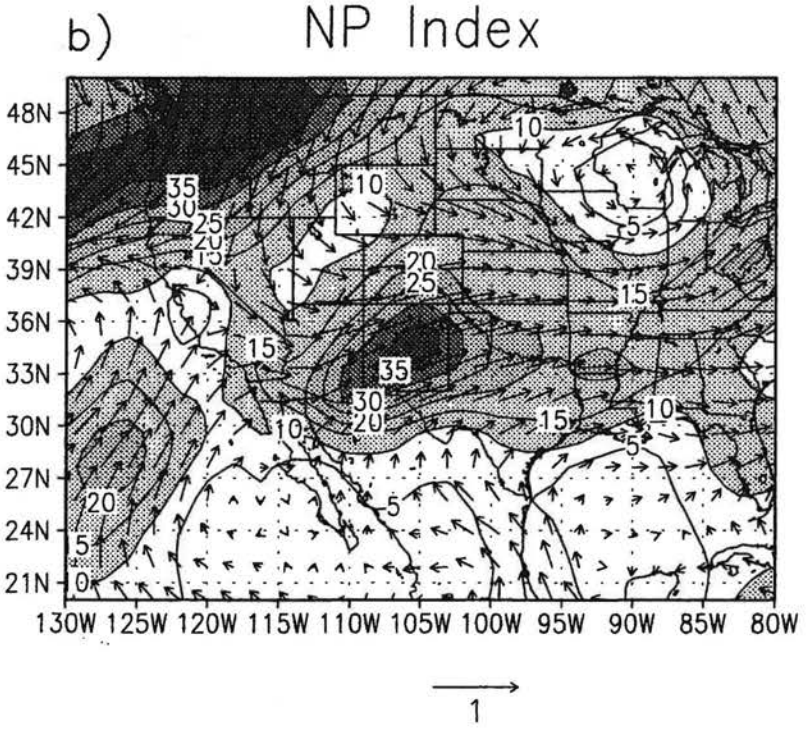

Figure 16. a) and b)

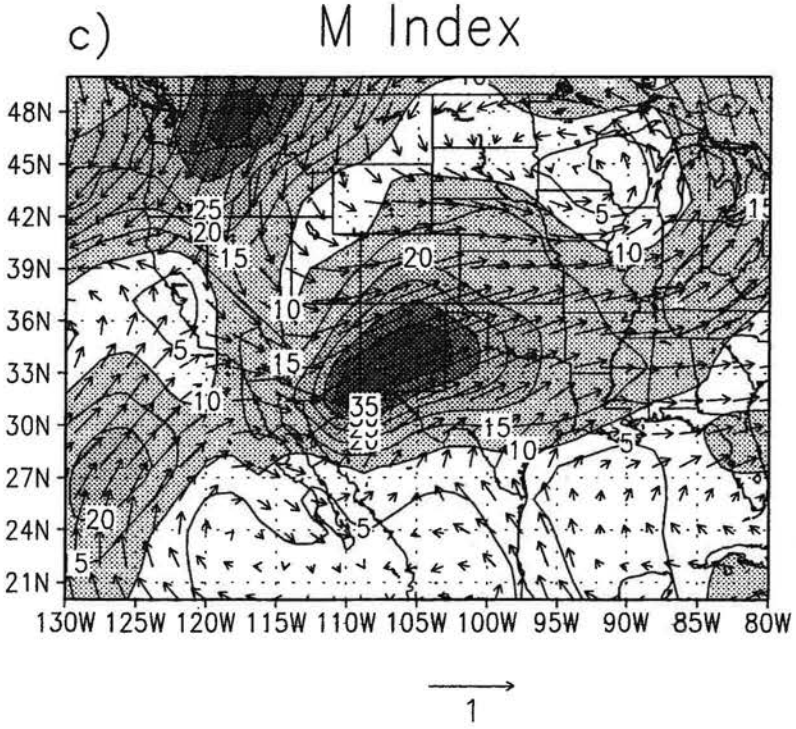
c)
M Index
48N
45N
42N
39N
36N
33N
30N
27N
24N
21N
130W 125W 120W 115W 110W 105W 100W 95W 90W 85W 80W
1

Figure 16. c)

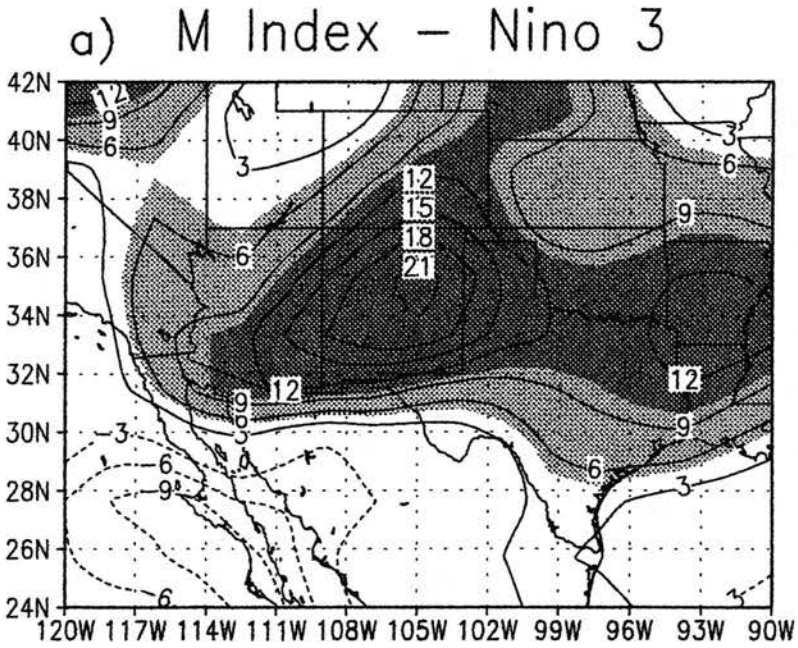

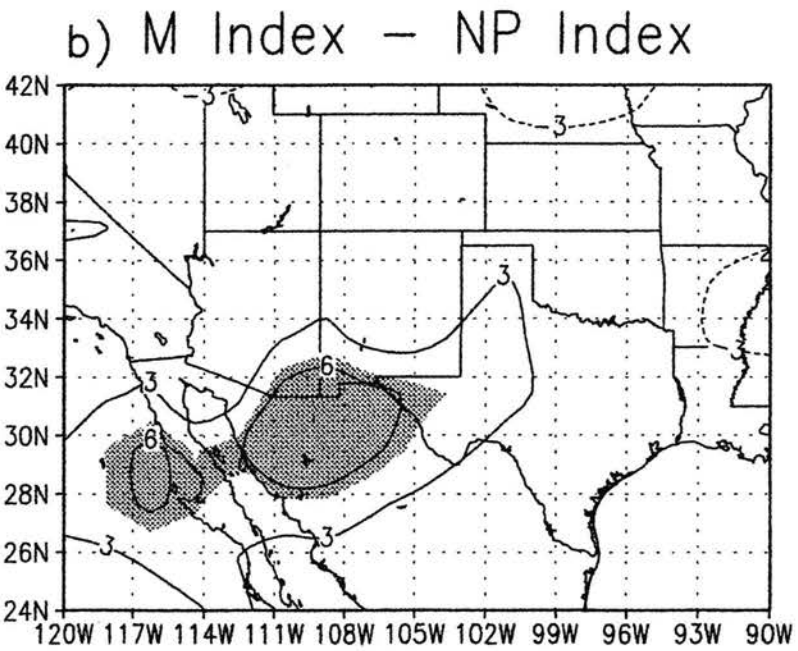

Figure 17. a) and b)

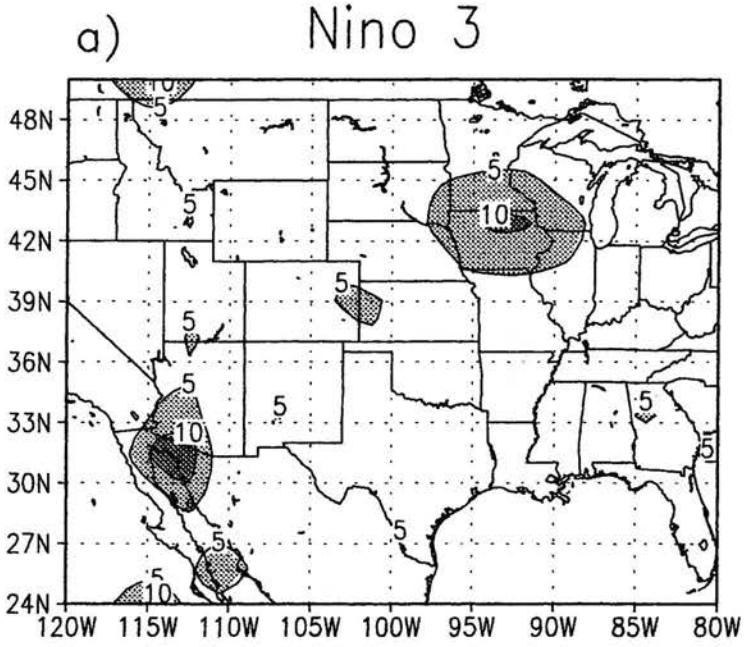

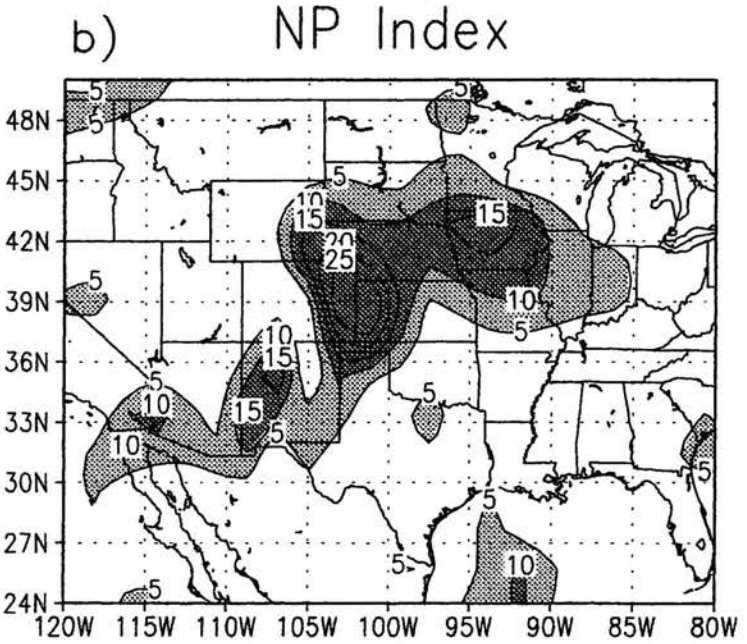

Figure 18. a) and b)

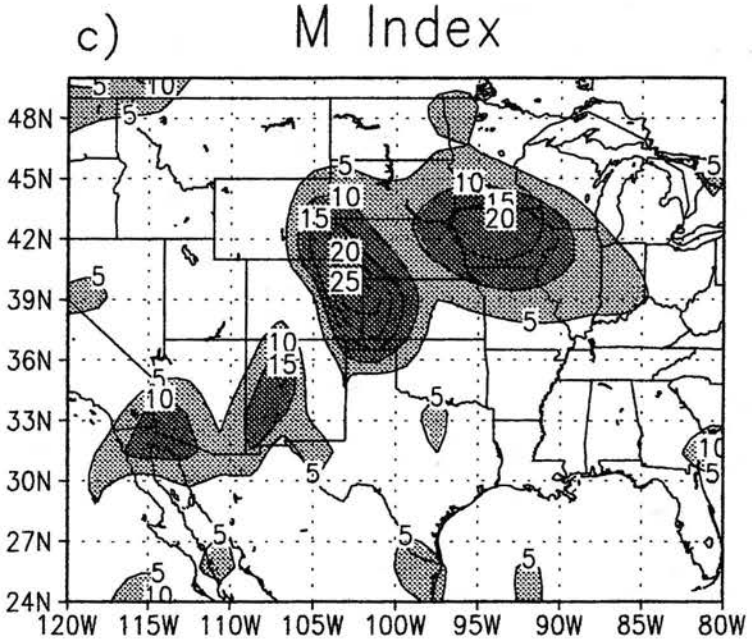
c)
M Index
48N
45N
42N
39N
36N
33N
30N
27N
24N
120W
115W
110W
105W
100W
95W
90W
85W
80W

Figure 18. c)

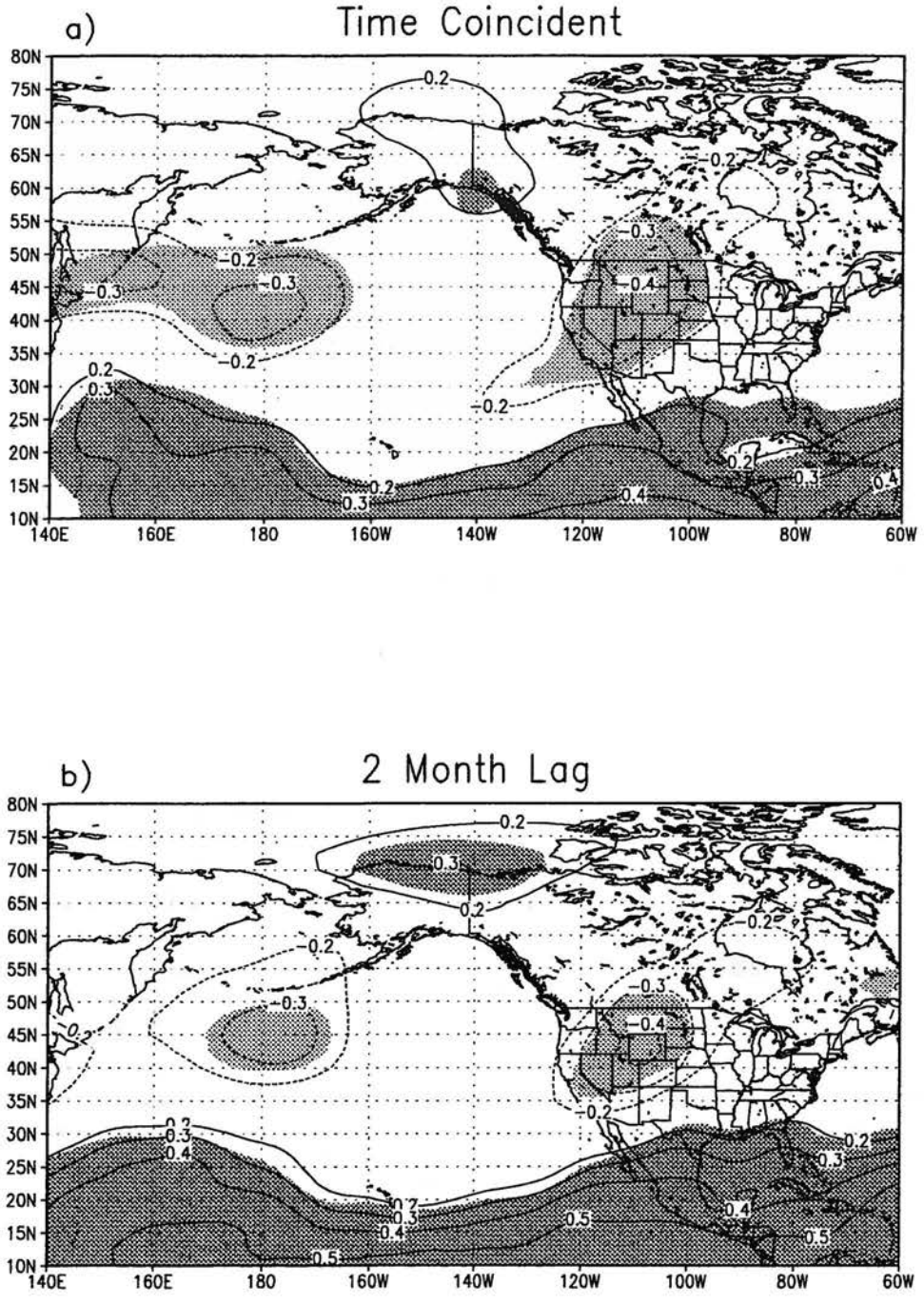

Figure 19. a) and b)

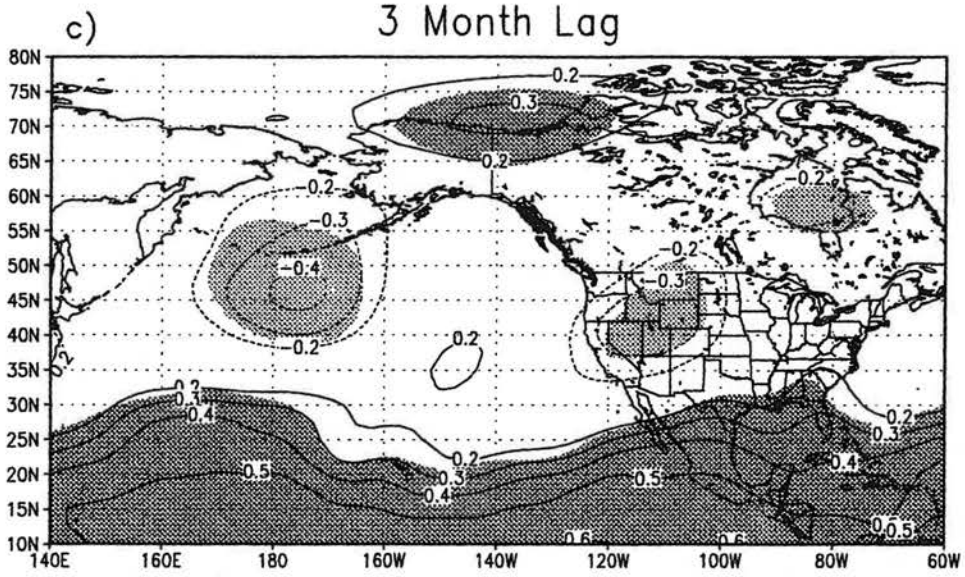

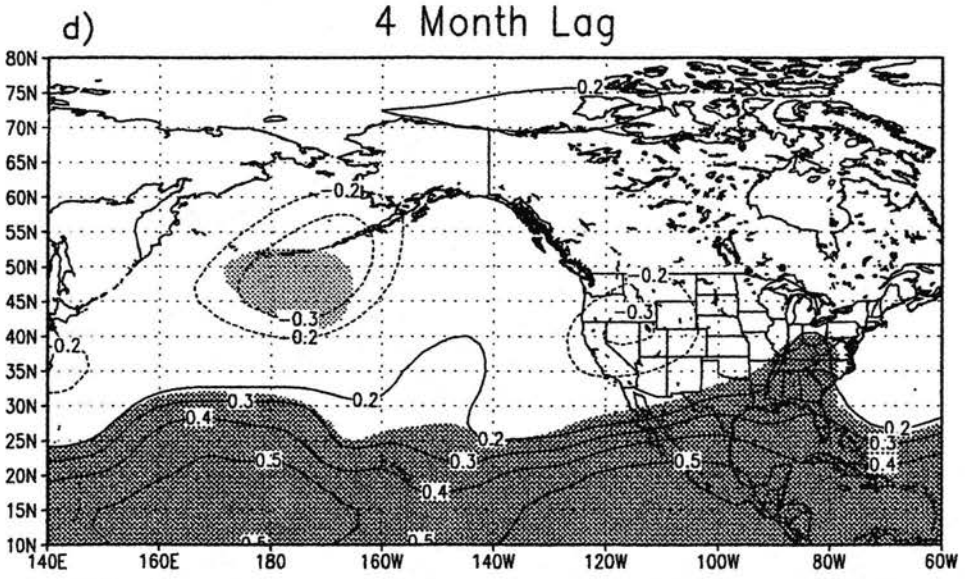

Figure 19. c) and d)

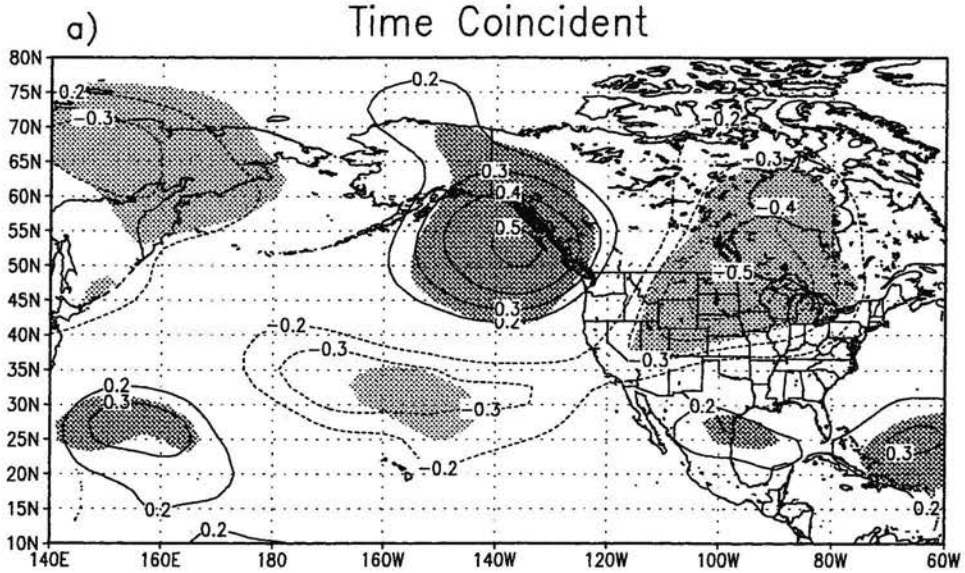
a)
Time Coincident
80N
75N
70N
65N
60N
55N
50N
45N
40N
35N
30N
25N
20N
15N
10N
140E
160E
180
160W
140W
120W
100W
80W
60W

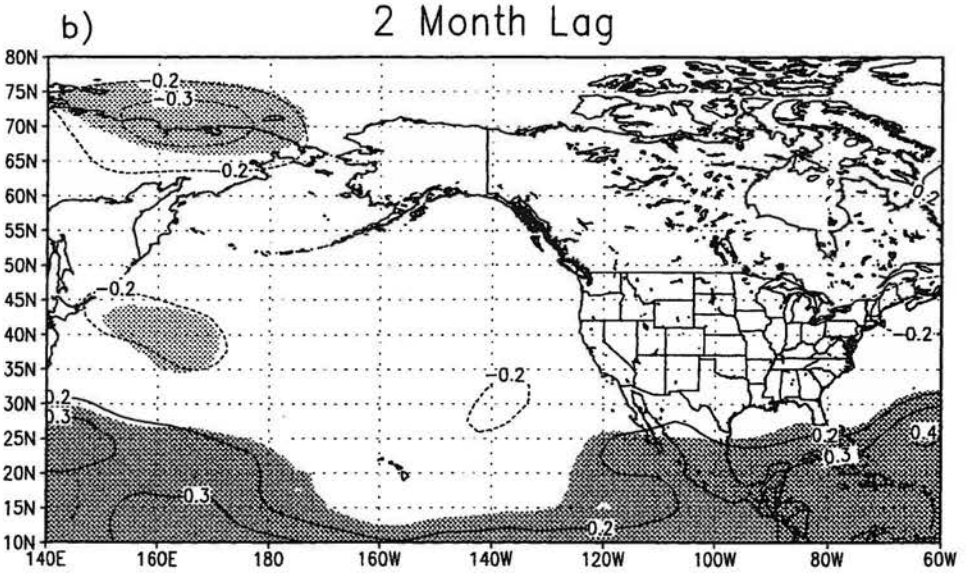
b)
2 Month Lag
80N
75N
70N
65N
60N
55N
50N
45N
40N
35N
30N
25N
20N
15N
10N
140E
160E
180
160W
140W
120W
100W
80W
60W

Figure 20.

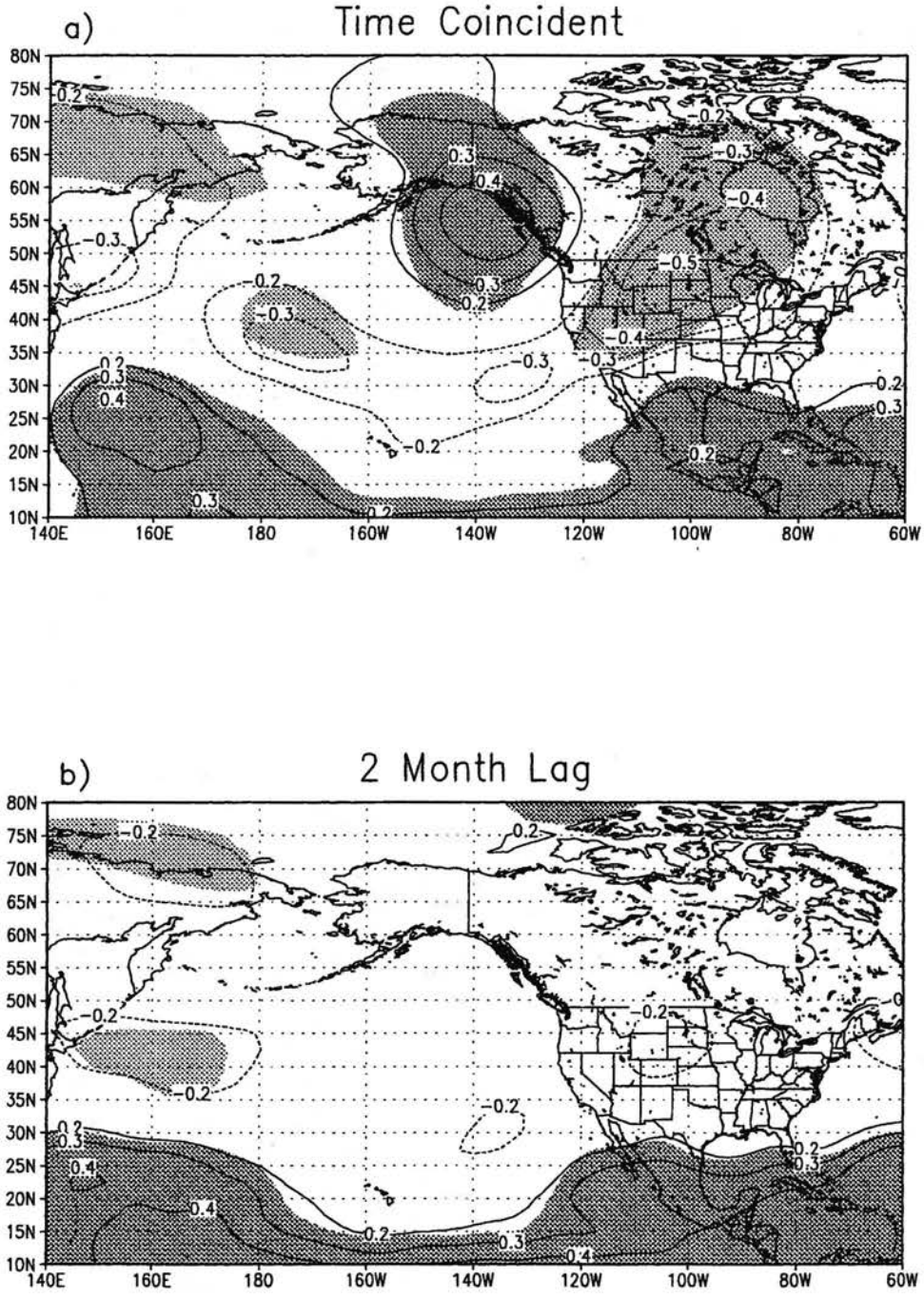
a)
Time Coincident
b)
2 Month Lag
80N
75N
70N
65N
60N
55N
50N
45N
40N
35N
30N
25N
20N
15N
10N
140E
160E
180
160W
140W
120W
100W
80W
60W

Figure 21.

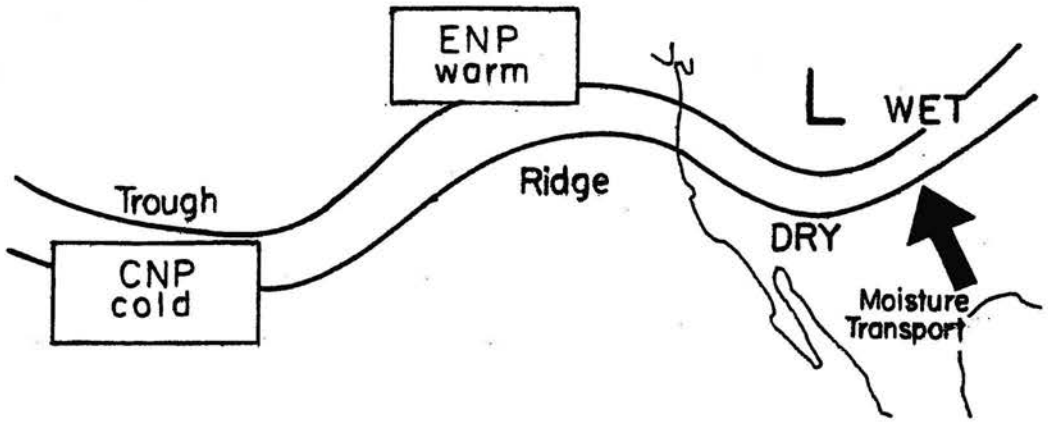

El Niño

M Positive
El Niño
High NPO Phase

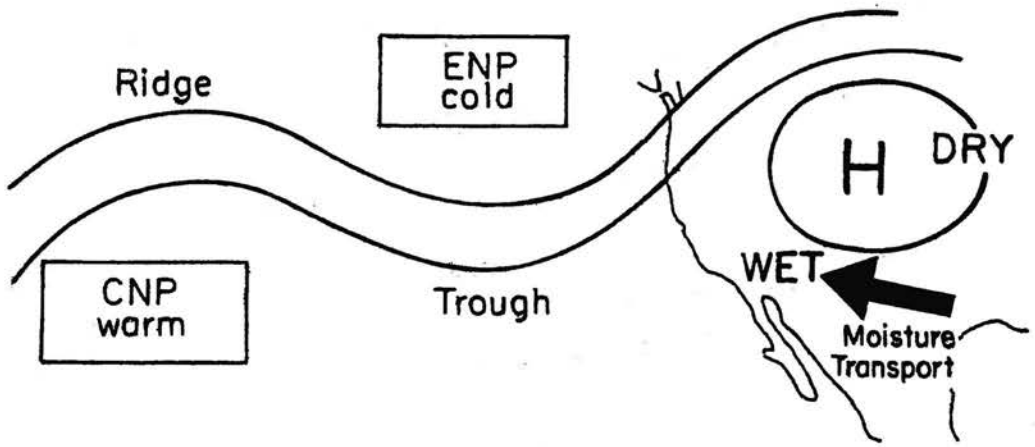

La Niña

M Negative
La Niña
Low NPO Phase

Figure 22.